NAVAL POSTGRADUATE SCHOOL

MONTEREY, CALIFORNIA

THESIS

ANGULAR RATE ESTIMATION BY MULTIPLICATIVE KALMAN FILTERING TECHNIQUES

by

Vincent C. Watson

December 2003

Thesis Advisor: Roberto Cristi
Co-Advisor: Brij Agrawal

Approved for Public Release; Distribution is Unlimited

THIS PAGE INTENTIONALLY LEFT BLANK

REPORT DOCUMENTATION PAGE			Form Approved OMB No. 0704-0188
Public reporting burden for this collection of information is estimated to average 1 hour per response, including the time for reviewing instruction, searching existing data sources, gathering and maintaining the data needed, and completing and reviewing the collection of information. Send comments regarding this burden estimate or any other aspect of this collection of information, including suggestions for reducing this burden, to Washington headquarters Services, Directorate for Information Operations and Reports, 1215 Jefferson Davis Highway, Suite 1204, Arlington, VA 22202-4302, and to the Office of Management and Budget, Paperwork Reduction Project (0704-0188) Washington DC 20503.			
1. AGENCY USE ONLY ***(Leave blank)***	**2. REPORT DATE** December 2003	**3. REPORT TYPE AND DATES COVERED** Master's Thesis	
4. TITLE AND SUBTITLE: Mitigation of Spacecraft Attitude Estimation Error Via Kalman Filtering			**5. FUNDING NUMBERS**
6. AUTHOR(S) Vincent C. Watson			
7. PERFORMING ORGANIZATION NAME(S) AND ADDRESS(ES) Naval Postgraduate School Monterey, CA 93943-5000			**8. PERFORMING ORGANIZATION REPORT NUMBER**
9. SPONSORING /MONITORING AGENCY NAME(S) AND ADDRESS(ES) N/A			**10. SPONSORING/MONITORING AGENCY REPORT NUMBER**
11. SUPPLEMENTARY NOTES The views expressed in this thesis are those of the author and do not reflect the official policy or position of the Department of Defense or the U.S. Government.			
12a. DISTRIBUTION / AVAILABILITY STATEMENT Approved for Public Release; Distribution is Unlimited			**12b. DISTRIBUTION CODE**

13. ABSTRACT (maximum 200 words)

Spacecraft attitude estimation and pointing accuracy have always been limited by imperfect sensors. The rate gyroscope is one of the most critical instruments used in spacecraft attitude estimation and unfortunately historical trends show this instrument degrades significantly with time. Degraded rate gyroscopes have impacted the missions for several NASA and ESA spacecraft, including the Hubble Telescope. A possible solution to this problem is using a mathematically modeled dynamic gyroscope in lieu of a real one. In this thesis, data from such a gyro is presented and integrated into a spacecraft attitude estimation algorithm.

The impediment to spacecraft attitude estimation presented by imperfect sensors has been overcome by developing more accurate sensors and using Kalman filters to reduce the effect of noisy measurements. Kalman filters for spacecraft attitude estimation have historically been based on an Euler angle or quaternion formulation. Though Euler angles and quaternions are arguably the easiest methods with which to describe the attitude of a spacecraft, other methods of describing attitudes do exist – including the Gibbs and Rodriguez parameters. A Kalman filter based upon the Gibbs parameter is presented and analyzed in this thesis.

14. SUBJECT TERMS Kalman Filter, Gibbs Parameter, Dynamic Gyroscope, Attitude Estimation			**15. NUMBER OF PAGES** 70
			16. PRICE CODE
17. SECURITY CLASSIFICATION OF REPORT Unclassified	**18. SECURITY CLASSIFICATION OF THIS PAGE** Unclassified	**19. SECURITY CLASSIFICATION OF ABSTRACT** Unclassified	**20. LIMITATION OF ABSTRACT** UL

NSN 7540-01-280-5500

Standard Form 298 (Rev. 2-89)
Prescribed by ANSI Std. 239-18

THIS PAGE INTENTIONALLY LEFT BLANK

Approved for Public Release; Distribution is Unlimited

ANGULAR RATE ESTIMATION BY MULTIPLICATIVE KALMAN FILTERING TECHNIQUES

Vincent C. Watson
Lieutenant, United States Navy
B.S., Georgia Institute of Technology, 1994

Submitted in partial fulfillment of the
requirements for the degree of

MASTER OF SCIENCE IN ASTRONAUTICAL ENGINEERING

from the

NAVAL POSTGRADUATE SCHOOL
December 2003

Author: Vincent C. Watson

Approved by: Roberto Cristi
Thesis Advisor

Brij N. Agrawal
Co-Advisor

Anthony J. Healey
Chairman, Department of Mechanical and Astronautical Engineering

THIS PAGE INTENTIONALLY LEFT BLANK

ABSTRACT

Spacecraft attitude estimation and pointing accuracy have always been limited by imperfect sensors. The rate gyroscope is one of the most critical instruments used in spacecraft attitude estimation and unfortunately historical trends show this instrument degrades significantly with time. Degraded rate gyroscopes have impacted the missions for several NASA and ESA spacecraft, including the Hubble Telescope. A possible solution to this problem is using a mathematically modeled dynamic gyroscope in lieu of a real one. In this thesis, data from such a gyro is presented and integrated into a spacecraft attitude estimation algorithm.

The impediment to spacecraft attitude estimation presented by imperfect sensors has been overcome by developing more accurate sensors and using Kalman filters to reduce the effect of noisy measurements. Kalman filters for spacecraft attitude estimation have historically been based on an Euler angle or quaternion formulation. Though Euler angles and quaternions are arguably the most common methods with which to describe the attitude of a spacecraft, other methods of describing attitudes do exist – including the Gibbs and Rodriguez parameters. A Kalman filter based upon the Gibbs parameter is presented and analyzed in this thesis.

THIS PAGE INTENTIONALLY LEFT BLANK

TABLE OF CONTENTS

LIST OF FIGURES

THIS PAGE INTENTIONALLY LEFT BLANK

ACKNOWLEDGMENTS

The author would like to thank several people for their contributions and support of this endeavor. Dr. Roberto Cristi first introduced me to the concept of mathematical filtering during my second quarter at the Naval Postgraduate School and provided me with vast insight and inspiration throughout the course of my study. Professor Barry Leonard provided me the knowledge base with which to apply Kalman Filtering to spacecraft attitude estimation. A special thank you is in order for Mr. Don Kolve of the Boeing Corporation, who taught me an unimaginable amount of information about spacecraft attitude estimation theory and practical engineering application. Dr. Brij Agrawal introduced me to the concept of a pseudo-gyroscope and guided my study of engineering in more aspects than I can recall. All of the above and many others have my undying thanks and gratitude.

THIS PAGE INTENTIONALLY LEFT BLANK

I. INTRODUCTION

A. SPACECRAFT ATTITUDE ESTIMATION

The pointing accuracy requirements of modern Department of Defense satellites have increased steadily over the past few decades. As the pointing accuracy requirements for a satellite increase, so does the level of accuracy in the estimation of its attitude. Spacecraft attitude estimation is an extremely complex and non-linear process. Inputs from several different sensors – such as star trackers and rate gyroscopes, among others – are required to determine the attitude of a spacecraft. Because no sensor is error-free – even at the time of manufacture – and all man-made equipment degrades with age, the problem of accurate attitude estimation throughout the mission life of a satellite is extremely important. A method for overcoming these impediments via a Kalman filtering process is presented and analyzed here.

Kalman filtering has been used in spacecraft attitude estimation for quite some time. The earliest published application was in 1970 by Farrell and several others have followed since. Lefferts, Shuster, and Markley published a thorough review of the topic in 1982 and since then Markley, Crassidis, and several others have kept Kalman filtering an active topic of research in the space industry [Markley]. Several different attitude representations have been used in Kalman filtering with varying degrees of success. Palermo successfully implemented a Kalman filter using an Euler angle representation of the attitude for a simulated bifocal relay mirror spacecraft [Palermo] and his dynamic model is used as a starting point for this work.

B. SATELLITE ENVIRONMENT

The environment in which a satellite operates complicates the problem of spacecraft attitude estimation and control. A satellite in orbit is subject to non-constant external torques at all times – some secular (varying linearly with time), some periodic, and some random. The forces that induce these torques are gravity gradient, magnetic, solar pressure, and atmospheric drag, though the effects of atmospheric drag on satellites outside of LEO is considered negligible. Though these torques can be predicted with high accuracy (with the exception of atmospheric drag), any errors in prediction couple with errors in sensor accuracy to increase the error in attitude estimation. Because large

errors in attitude can be attributed to the effects of these external torques, a brief overview of gravity gradient, magnetic, and solar torque and the errors that can result from each is presented here. For more in depth information the reader is referred to texts by Sidi, Bong Wie, or Hughes [Sidi, Bong Wie, Hughes]. In the rest of this section we survey a number of disturbances acting on the spacecraft.

1. Gravity Gradient Torque

A spacecraft is not a point mass and may not be treated as such. It is a rigid body (in most cases) with a mass distribution about a center of mass. Vice treating it as a point mass an inertia dyadic is used. Gravity gradient torques are imparted to a spacecraft because gravity acts on each element of the spacecraft. Gravity acting on a mass *m* located at a distance *r* from the spacecraft center of mass will induce a torque about the center of mass. The effects of gravity will act on each portion of the satellite in accordance with Newton's Laws of Gravitation. Ignoring the effects of the moon and other third bodies due to their small effects, these torques may be written as:

$$\vec{N}_{GG} = \frac{3\mu}{R_0^3}\hat{R}_{0_B} \times (I_B \cdot \hat{R}_{0_B}) \qquad (1\text{-}1)$$

where μ is the gravitational parameter for the Earth, $\hat{R}_{0_B}$ is the distance from the satellite to the center of the Earth, and I_B is the inertia dyadic for the satellite.

Some satellites with low pointing requirements actually use gravity gradient stabilization. A quick examination of equation 1-1 reveals that knowledge of the position of the satellite and the inertia dyadic are critical for predicting the gravitational torque. System identification algorithms are being actively researched and developed to facilitate more precise knowledge of spacecraft inertia dyadics.

In addition to its own mass distribution, the fact that the gravitational field produced by the Earth is an aspherical potential further complicates the problem. Like a satellite, the Earth does not have a uniform mass distribution – hence its aspherical gravity field. Zonal, tesseral, and sectoral harmonics within the field are both non-linear and extremely complex to model mathematically. Inaccuracies in modeling the gravitational field of the Earth can lead to attitude pointing errors as well.

2. Magnetic Torque

The Earth has a rotating magnetic field $\vec{B}$ through which any orbiting satellite must travel. The satellite itself has an intrinsic magnetic moment $\vec{m} = \begin{bmatrix} m_x \\ m_y \\ m_z \end{bmatrix}$. Interaction between the magnetic moment of the spacecraft and the magnetic field of the Earth generates a torque on the spacecraft calculated by

$$\vec{N}_B = \vec{m} \times \vec{B} \qquad (1\text{-}2)$$

The magnitude of $\vec{B}$ will decrease as the satellite altitude increases. For dealing with torques induced by the interaction of the spacecraft and Earth magnetic fields, precise knowledge of the spacecraft magnetic moment $\vec{m}$ is critical. As with the moment of inertia, system identification algorithms can be used to mitigate errors due to inaccurate estimates of $\vec{m}$.

3. Solar Torque

Maxwell's equations imply that electromagnetic waves have momentum, which may be transferred to objects with which it comes in contact. Since light is an electromagnetic wave, it exerts pressure. Though this pressure is miniscule in an Earth environment it is not miniscule for a satellite in orbit about the Earth.

For electromagnetic radiation, basic physics shows us that *Electromagnetic Force = Work + Energy Density* which, when expressed in a more mathematical manner becomes

$$\int_S (T \cdot d\vec{a}) d\vec{a} = \int_V F dV + \frac{\partial}{\partial t} \int_V \frac{\vec{S}}{c^2} dV \qquad (1\text{-}3)$$

where T is the Maxwell stress tensor, F is the force density, and $\vec{S}$ is the Poynting vector ($\vec{S} = \frac{c}{4\pi} \vec{E} \times \vec{B}$).

The amount of pressure exerted on an object by an electromagnetic wave is highly dependent upon the type of surface being illuminated. In some complex models, the type of reflection – specular or diffuse – as well as the reflectivity of the surface plays a part in

the calculation. In a simple model the following equation is often used to determine the maximum solar torque imparted to a spacecraft

$$\left|\vec{N}_{SP}\right| = \frac{F_S}{c} A_S (1+q)\cos(i)(c_{sp} - c_g) \qquad (1\text{-}4)$$

where A_S is the spacecraft area, q is the reflectance factor, i is the angle of incidence of the incoming light, $c_{sp} - c_g$ is the distance between the spacecraft center of gravity and the center of solar pressure, and F_S is the solar power density (which varies with time). Solar cycles, changes in $c_{sp} - c_g$ due to fuel expenditures, and the changing area of a spacecraft tracking a point on the Earth all contribute to the difficulty of estimating and compensating for disturbances due to solar pressure [SMAD].

4. Atmospheric Drag

As previously mentioned the effects of atmospheric drag on satellites outside of LEO are considered negligible. For LEO satellites, however, atmospheric drag is the most difficult external torque to predict. Because the dynamics of the outer reaches of the atmosphere are not fully understood it cannot be modeled accurately. The effects of drag on LEO spacecraft are directly proportional to the area of the spacecraft. Atmospheric drag, though pertinent to LEO applications, was not included in any of the models used in developing this thesis but is mentioned here for completeness.

C. SENSORS

Accurate measurement of data from external sources is required for a spacecraft attitude control system to estimate its attitude. Though several sensors exist that perform this function – including sun sensors, horizon sensors, and earth sensors among others – the star tracker is the most accurate and pertinent to the focus of this work.

1. Rate Gyroscopes

A cursory perusal of either the Euler Equations of Motion or the kinematic equations for the quaternion or Gibbs parameters reveals their dependence upon angular rate data. Any error in angular rate measurement or calculation will result in an error in spacecraft attitude estimation. Angular rate information is critical to the accurate estimation of spacecraft attitude – regardless of the estimation method. Rate gyroscopes provide this information to the spacecraft attitude control system.

There are several different kinds of rate gyroscopes available for use in the space environment today. Mechanical rate gyroscopes and rate integrating gyroscopes have been in use on orbit for quite several years. Both of these types of gyroscopes are dependent upon mechanical moving parts which degrade over time. Laser gyroscopes, quartz rate sensors, and hemispherical resonator gyroscopes are now available today with much higher accuracies and no reliance on moving parts [Sidi].

2. Dynamic Gyroscopes

Rate gyroscopes are man-made devices and therefore have finite lifetimes – especially in the harsh environs of space. Because all of the external secular and periodic torques on a spacecraft may be modeled with some modicum of accuracy and the torques applied to the spacecraft via the momentum exchange devices of its attitude control system are known with a fair amount of precision, it is possible to determine the angular rate of the spacecraft via mathematical modeling and the use of external measurements. Such an algorithm is called a dynamic gyroscope. The use of a dynamic gyroscope upon failure of a simulated mechanical gyroscope is shown and analyzed in this work.

3. Star Trackers

Navigators from ancient times used the stars as navigational aids. Satellites navigating in space do the same via a device called a star tracker. Because stars may be considered inertially fixed bodies for all intents and purposes and because they are extremely small as seen from our solar system, they are ideal objects to use as an attitude reference. Star trackers provide the most accurate attitude data to the spacecraft attitude control system by several orders of magnitude over any other type of sensor. While older star trackers were capable of tracking only one star at a time, the new generation of star trackers can feed attitude quaternions to its host satellite and track multiple stars simultaneously. A new type of star sensor is currently being developed by Dr. Junkins et al which will use two simultaneous images of star fields from different parts of the sky to determine spacecraft attitude [Junkins].

D. KALMAN FILTERS

As previously mentioned, a satellite attitude control system receives input from imperfect external sensors to estimate the actual attitude of the satellite. The Kalman filter is an estimation algorithm frequently employed to do this. In essence, the Kalman

filter is a set of mathematical equations that provides a recursive solution of the least-squares estimation method. It supports computational estimations of past, present, and future states and can do so even when the nature of the system under consideration is not precisely known.

Given the extremely non-linear and varying nature of the space environment, this makes it an ideal tool with which to perform spacecraft attitude estimation. The effectiveness of the filtering algorithm is highly dependent upon how the state vector is defined, the type of filter employed, and several other factors. In this research we developed a Kalman Filter based on specific parameterization of the spacecraft attitude and attitude error.

E. STAR GAPS AND RATE GYROSCOPE UPSETS

Satellites in orbit currently experience periods in which their star trackers are unable to sense stars – called star gaps. Rate gyroscopes in some older satellites are sometimes sending data over 1000 times the actual reading – such an event is called a rate gyroscope upset. Both of these events wreak havoc upon attitude control algorithms - the Kalman filter in particular. Both of these phenomena are simulated and their effects mitigated via adaptive covariance and dynamic gyroscope integration.

F. THESIS ORGANIZATION

In this thesis we introduce the dynamics of spacecraft attitude in Chapter Two. Chapter Three begins with a cursory overview of the Kalman filtering process followed by a brief section on attitude error representation. It closes with a derivation of the Gibbs parameter based Kalman filter. Chapter Four covers the problems caused by star gaps and methods of managing such problems. Chapter Five introduces the dynamic gyroscope and methods of dealing with rate gyroscope upsets.

II. SPACECRAFT ATTITUDE

A. ATTITUDE PARAMATRIZATON

In this section we review spacecraft attitude estimation methods. There are several methods for doing this, but only a short description of most of them will be included here. Emphasis will be placed on the quaternion because understanding the quaternion is critical to comprehending the development of the Kalman filters used in spacecraft attitude estimation.

Regardless of the method, describing the attitude of a spacecraft basically entails describing the orientation of one coordinate system with respect to another. For purposes of satellites, a coordinate system based on the principal axes of the spacecraft – called the body coordinate system – and Earth Centered Inertial (ECI) systems are used.

1. Direction Cosine Matrix

The direction cosine matrix is the simplest manner in which to describe the attitude of a spacecraft. Given two coordinate systems each consisting of three orthogonal unit vectors there exists a three by three matrix C that relates the two coordinate systems.

When dealing with different coordinate systems it becomes necessary to develop a notation for annotating in which coordinate system a vector is expressed. In this paper a superscript to the left of the vector will indicate the coordinate system in which a vector is expressed. For example, ${}^{i}\vec{v}$ is a vector in the inertial reference frame while ${}^{b}\vec{v}$ is a vector in the body reference frame.

A vector ${}^{b}\vec{x} = \begin{bmatrix} x \\ y \\ z \end{bmatrix}$ expressed in body coordinates may be expressed in inertial coordinates by multiplying it by a direction cosine matrix (DCM) as shown below

$$ {}^{i}C^{b}\,{}^{b}\vec{x} = {}^{i}\vec{x} \qquad (2\text{-}1) $$

Note the two superscripts on the DCM. For a direction cosine matrix, the superscript on the left indicates the coordinate system the DCM transforms a vector *to*

while the right superscript indicates the coordinate system *from* which the vector is being transformed. Conversely, a vector in the inertial frame may be expressed in body frame coordinates by

$$ {}^{b}C^{i}\,{}^{i}\vec{x} = {}^{b}\vec{x} \qquad (2\text{-}2) $$

As one might expect ${}^{i}C^{b}$ and ${}^{b}C^{i}$ are related as the transpose of each other.

2. Euler Angles

Euler angles are a series of rotations about the axes of one coordinate system to align it to another coordinate system. These rotations are sometimes referred to as roll φ (rotation about the *x* axis), pitch θ (rotation about the *y* axis), and yaw ψ (rotation about the *z* axis).

Since in the Euler angle formulation the order matters, there are twelve possible combinations of Euler angles one may use to go from one coordinate system to another. Multiplication of the individual rotation matrices for each Euler angle will result in a direction cosine matrix. Given the two coordinate systems *a* and *b* the direction cosine matrix for a roll-pitch-yaw Euler sequence would be

$$ {}^{a}C^{b} = \begin{bmatrix} 1 & 0 & 0 \\ 0 & \cos\varphi & \sin\varphi \\ 0 & -\sin\varphi & \cos\varphi \end{bmatrix} \begin{bmatrix} \cos\theta & 0 & -\sin\theta \\ 0 & 1 & 0 \\ \sin\theta & 0 & \cos\theta \end{bmatrix} \begin{bmatrix} \cos\psi & \sin\psi & 0 \\ -\sin\psi & \cos\psi & 0 \\ 0 & 0 & 1 \end{bmatrix} \qquad (2\text{-}3) $$

3. Quaternions

A mathematical structure called the quaternion is a convenient method with which to describe the orientation of a coordinate system.

a. Quaternion Definition

Quaternions are a form of hyper-complex numbers invented by William Hamilton in the nineteenth century and are today used extensively both in robotics and spacecraft attitude control. Quaternions are represented as a four element set consisting of three vector components and one scalar component

$$q = \begin{bmatrix} q_1 \\ q_2 \\ q_3 \\ q_4 \end{bmatrix} \qquad (2\text{-}4)$$

There is no set convention for which element of the quaternion is a scalar, but in this paper q_4 will always be the scalar element of the quaternion.

b. Attitude Quaternions

When used for describing an attitude, quaternions are constrained to the surface of a four dimensional hyper-sphere defined by

$$q_1^2 + q_2^2 + q_3^2 + q_4^2 = 1 \qquad (2\text{-}5)$$

To determine the physical meaning of quaternions constrained on this hyper-sphere, consider two coordinate systems as shown below, S and S'. The vector portion of the quaternion represents an axis about which coordinate system *S* must be rotated to align it with the *S*'coordinate system – called the eigenaxis.

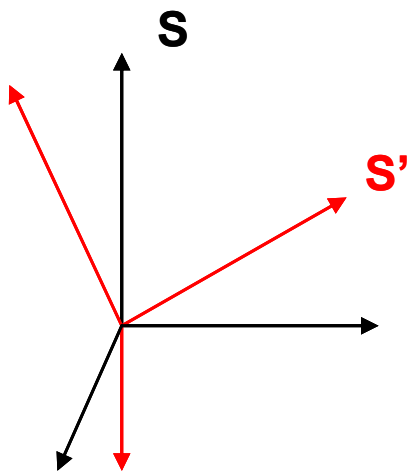

Figure 1. Coordinate Systems S and S'

The scalar portion of the quaternion is a measure of the magnitude of the rotation θ_r. Defining the eigenaxis as a unit vector $\vec{e} = \begin{bmatrix} e_x \\ e_y \\ e_z \end{bmatrix}$, the quaternion elements may be defined as follows:

$$\begin{aligned} q_1 &= \sin\left(\frac{\theta_r}{2}\right) e_x \\ q_2 &= \sin\left(\frac{\theta_r}{2}\right) e_y \\ q_3 &= \sin\left(\frac{\theta_r}{2}\right) e_z \\ q_4 &= \cos\left(\frac{\theta_r}{2}\right) \end{aligned} \qquad (2\text{-}6)$$

Since quaternions are vectors of unit magnitude, they may not be added together through the standard definition of addition. Quaternion algebra is a rich and interesting topic, but one that will not be dealt with here in its entirety. Two uses of quaternion algebra will be addressed because of their usefulness in attitude estimation – the quaternion conjugate and quaternion multiplication.

c. The Quaternion Conjugate

The quaternion conjugate of quaternion q is given by

$$q^* = -q_1 - q_2 - q_3 + q_4 \qquad (2\text{-}7)$$

From a physical standpoint, the conjugate of a quaternion q represents a rotation of the same magnitude about a vector in the opposite direction. It is also worthy to note that the inverse of a quaternion is identical to its complex conjugate. The quaternion conjugate is useful when using the quaternion as a rotation operator, which will be discussed later.

d. Quaternion Multiplication

As noted previously, quaternions have their own unique algebra. The symbol $\otimes$ is used to denote quaternion multiplication. It can be shown that the quaternion product is defined by

$$p \otimes q = \begin{bmatrix} q_4 & q_3 & -q_2 & q_1 \\ -q_3 & q_4 & q_1 & q_2 \\ q_2 & -q_1 & q_4 & q_3 \\ -q_1 & -q_2 & -q_3 & q_4 \end{bmatrix} \begin{bmatrix} p_1 \\ p_2 \\ p_3 \\ p_4 \end{bmatrix} \qquad (2\text{-}8)$$

which may also be written as

$$p \otimes q = \begin{bmatrix} p_4 q + q_4 p - \vec{p} \times \vec{q} \\ p_4 q_4 - \vec{p} \square \vec{q} \end{bmatrix} \qquad (2\text{-}9)$$

The quaternion product is a useful tool for time propagation of the quaternion – as will be shown later. Recall that a quaternion represents a rotation from a reference frame to a given attitude. It naturally follows that the quaternion product defined in equation 2-9 would also represent a rotation – which it does. Defining $A(q)$ as a DCM representing the same rotation as quaternion *q*, it may be shown that

$$A(p \otimes q) = A(p)A(q) \qquad (2\text{-}10)$$

e. Quaternion Propagation

Given an angular velocity vector $\vec{\omega}$ in body coordinates and an initial orientation expressed by the quaternion q_0 the orientation at any time *t* may be expressed as the solution of the following differential equation

$$\frac{dq}{dt} = \dot{q} = \frac{1}{2} \begin{bmatrix} \vec{\omega} \\ 0 \end{bmatrix} \otimes q \qquad (2\text{-}11)$$

with the initial condition $q(0) = q_0$.

f. Advantages of Quaternions

Quaternion representations of spacecraft attitude hold several advantages over the Euler angle and direction cosine matrix representations. Perhaps the most obvious advantage comes from the size - a quaternion is a four element structure, whereas a direction cosine matrix has nine elements. A quaternion describes the same attitude with half of the number of elements, saving both memory and processing power. The simplicity of the time derivative of the quaternion makes it an ideal method with which to do attitude propagation. Also of great importance is the fact that it has no singularities.

4. Gibbs Vector

Gibbs vectors are closely related to quaternions, though they exist in $\mathbb{R}^3$ vice $\mathbb{R}^4$. The Gibbs vector is defined as

$$\vec{g} = \frac{1}{q_4}\begin{bmatrix} q_1 \\ q_2 \\ q_3 \end{bmatrix} = \vec{e}\tan\left(\frac{\theta_r}{2}\right) \equiv \frac{a_g}{2} \qquad (2\text{-}12)$$

The Gibbs vector is obviously singular whenever q_4 goes to zero, which occurs for rotations of 180 degrees. Consequently, the Gibbs parameter is an extremely effective tool for describing rotations in the interval $(-180^\circ, +180^\circ)$. The relationship between the Gibbs vector and the quaternion is shown in the gnomonic projection in figure 2:

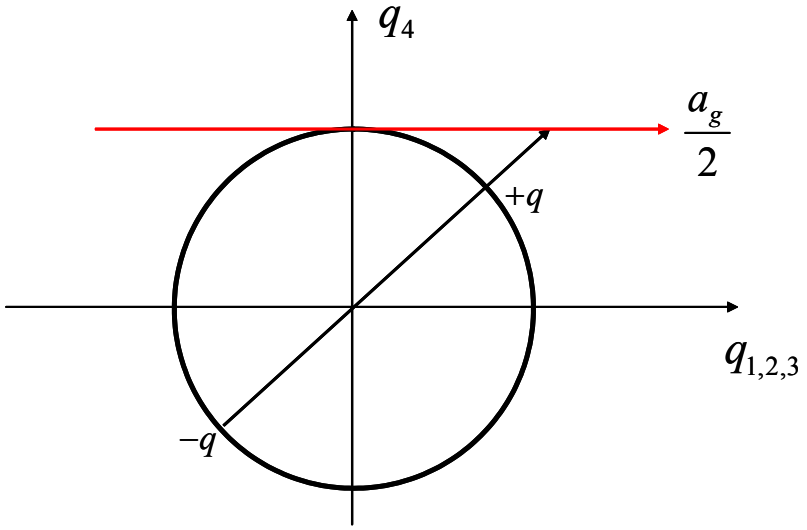

Figure 2. Gibbs vector as a Gnomonic Projection

B. ATTITUDE SENSORS

Measurement of external data is required in order to produce an attitude estimate. There are a multitude of sensors available to measure attitude data for a spacecraft, including horizon sensors, sun sensors (coarse and fine), and star trackers. None of these provides a perfect measurement, hence the need for attitude error estimation. A brief overview of rate gyroscopes and star trackers along with their respective sources of error is presented here, as both are simulated in models used in this thesis.

1. Rate Gyroscopes

Rate gyroscopes provide angular rate data to the spacecraft attitude control system. There are several different types of rate gyroscopes available today, including mechanical, fiber optic, laser, and hemispherical resonator gyroscopes. Regardless of the type of gyroscope, all perform the same function. Each sends the spacecraft attitude control system the angular rates of the satellite in body coordinates. It is beyond the scope of this work to describe each in detail, but one thing that all rate gyroscopes have in common is that they are inherently noisy. The errors sent to the attitude control system by noisy rate gyroscopes may be categorized into four distinct types of error: bias error, random walk, scale factor error, and orthagonality errors.

a. Bias

Bias error is sometimes referred to as a constant drift. Bias errors for current generation gyroscopes range from $0.001^\circ / \text{hour}$ to $1^\circ / \text{hour}$. The measured angular rate for a rate gyroscope may be expressed as

$$\omega_{meas}(t) = \omega(t) + b(t) \qquad (2\text{-}13)$$

With *b(t)* representing the bias at time *t*. As will be shown later in this work, it is possible to estimate gyroscope bias via a Kalman filtering process.

b. Rate Walk

Rate walk is sometimes described as bias drift. Random walk propagates from the white noise of the sensor and is responsible for non-deterministic behavior. Its units are normally $^\circ / \sqrt{hour}$.

c. Scale Factor

The scale factor error is the linear deviation of the measured rate from the true rate – normally given as a percentage or in parts per million. Asymmetry and non-linearity have been observed in scale factors for rate gyroscopes. Scale factors are caused by imperfections in manufacturing and the degradation of the gyroscope with the passage of time [Hewitson et al]. Though a source of error in any gyroscope, scale factors are not used in any of the models in this work, but are presented here for completeness.

d. Orthogonality Errors

Rate gyroscopes are mounted in clusters relative to one another to provide data to a spacecraft attitude control system. Any misalignment of the sensors with respect to one another will result in error – known as orthogonality error. Launch vibrations and thermal deformation over time could cause such errors to occur. As with scale factor errors, no orthogonality errors are modeled in this work – they are presented for theoretical completeness.

2. Star Trackers

As their name implies, star trackers generate attitude data based upon the relative position of stars as seen from the spacecraft itself. Each star sensor has a star catalog with which to compare the image it sees. Due to the large number of recorded stars, the exact composition of the catalog will be determined by the orbit in which the host satellite will be placed – there is no such thing as a standard star catalog.

a. Star Characteristics

In order to use stars for navigational purposes it is necessary to differentiate between stars. There are two characteristics of stars which make this possible – magnitude and spectra.

Magnitude refers to the brightness of a star. There are two types of magnitude – absolute and apparent. The apparent magnitude is how bright an object seems when viewed from the Earth. In contrast, the absolute magnitude is the apparent magnitude of an object placed at ten parsecs away. Star trackers use the apparent magnitude for their calculations.

The spectrum of a star refers to the type of radiation it is emitting. Stellar spectra are divided into seven categories. There are O, B, A, F, G, K, and M class stars, with O being the hottest and M being the coolest star.

b. Star Sensing

Current generation star trackers use Charge Coupled Devices (CCDs) to detect stars, though future generation star trackers will use CMOS technology [Junkins]. A stray light shield prevents light from outside the star tracker bore sight from reaching the CCD. Once the CCD has registered a star field image, the star sensor processor will match that image with its library and send an attitude quaternion to the spacecraft attitude

control system. This is an extremely simplified explanation of what actually occurs, but the actual mechanics of this process are outside the scope of this work.

c. Star Tracking

Once one or more stars have been acquired, the spacecraft will move around the Earth in its orbit and possibly change its attitude intentionally. The software must track the image of the star through this motion and be ready to acquire a new star when the image exits the Field of View (FOV) of the star tracker [Sidi].

d. Star Gaps

There are times when a star exits the field of view (FOV) of a star tracker and no new star within the new FOV has been acquired. During such time periods no data is being sent to the satellite attitude control system – such periods are called star gaps. Star gaps may also be caused by the satellite pointing in such a way that the moon or sun prevents the star tracker from sensing any stars due to their high intensity. Star gaps are detrimental to attitude determination when they extend for more than a few seconds and can wreak havoc on attitude estimation algorithms, as will be shown in a later section.

e. Star Tracker Error

Although easily the most accurate sensor available, star trackers are not error free. Like rate gyroscopes, star trackers also have a scale factor, which will vary with age. The CCD assemblies are temperature sensitive structures – a primary source of error. Misalignments of star trackers with respect to the spacecraft body as a result of launch vibration or thermal deformation over time are also a source of star tracker error.

THIS PAGE INTENTIONALLY LEFT BLANK

III. KALMAN FILTERING FOR ATTITUDE ESTIMATION

As shown in the preceding section, satellite attitude control systems estimate the attitude of the satellite based upon measurements from imperfect sensors. As time passes the sensors degrade and the data they send to the attitude control system degrades as well. The Kalman filter provides a solution to this problem. In this section the Kalman filter is introduced in its basic form. Attitude error representations are introduced and then a state vector is defined for attitude estimation purposes. A discrete Kalman filter for attitude estimation based upon the Gibbs parameter is then developed and the results of its implementation are presented.

A. THE KALMAN FILTER

As alluded to previously, a Kalman filter is a recursive mathematical algorithm that allows one to estimate the state of the system based upon its previous states, its known dynamics, and knowledge of the accuracies of the sensors involved. Once initialized, there are three steps to the filtering process: prediction, measurement, and correction. A diagram of these steps is shown below. There are two main types of Kalman filters – regular and extended. A brief overview of each is presented here.

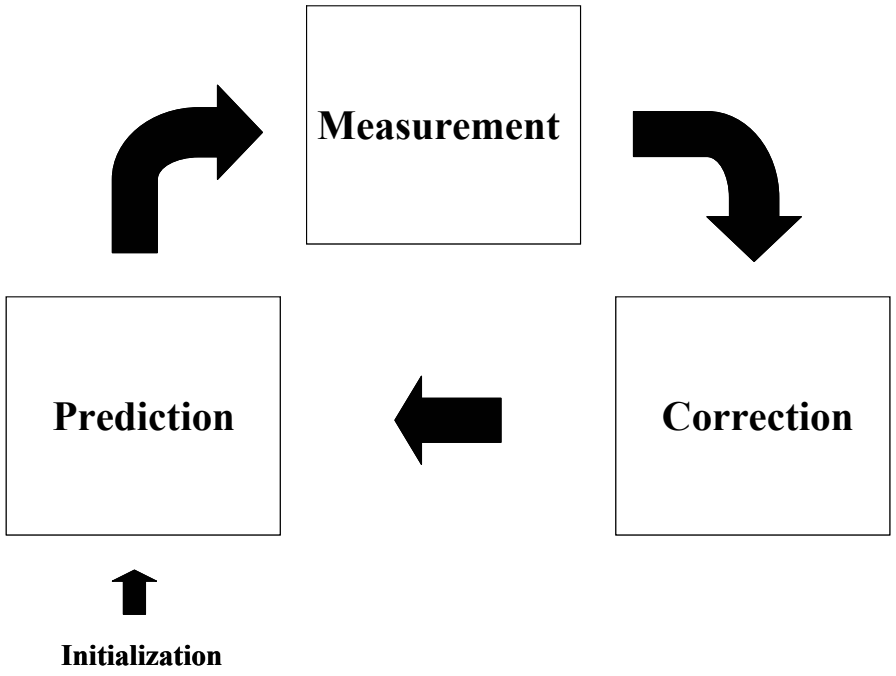

Figure 3. Kalman Filtering Process Diagram

1. The Kalman Filter

The Kalman filter may be used to predict the future state of a process governed by the following equation

$$x_{k+1} = F_k x_k + G u_k + w_k \qquad (3\text{-}1)$$

where k represents the time step and x is a vector of state variables $x \in \Re^n$. F_k is an $n \times n$ matrix known as the state transition matrix which relates the current state to the next one. The matrix G is a $n \times l$ matrix that relates the control input at time step k - u_k - to the state x. The final term w_k is the process or plant noise. This noise accounts for random inputs and inaccuracies of the state space model that cause the plant to perform in a non-deterministic manner. The noise is assumed to be white noise with a normal probability distribution

$$p(w) \square N(0, Q) \qquad (3\text{-}2)$$

where Q_k is a matrix representing the plant noise w defined by

$$Q_k \equiv \mathrm{cov}(w_k) \qquad (3\text{-}3)$$

Although the state vector represents all the variables being estimated, not all the estimated variables are required to be measured. The measurement is related to the state by the following equation

$$z_k = H_k x_k + v_k \qquad (3\text{-}4)$$

where H_k is an $m \times n$ matrix often referred to as the measurement matrix or the measurement sensitivity matrix in some cases. The second term v_k represents the measurement noise – or sensor inaccuracies. As with the plant noise, it is assumed to be white noise with a normal distribution given by

$$p(v_k) \square N(0, R_k) \qquad (3\text{-}5)$$

where R_k is the measurement error covariance matrix defined by

$$R_k \equiv \text{cov}(v_k) \qquad (3\text{-}6)$$

It is important to note that though they share a similar probability distribution, the plant and measurement noise are completely independent of one another. If a system under consideration can be described by equations 3-1 and 3-3, then a discrete Kalman filtering algorithm may be used to estimate its future states.

a. Prediction

The first phase of a filtering algorithm is the prediction phase. In this phase at time step k a prediction $\hat{x}_{k+1}$ is made for the next time step based upon the current state using the system model. This prediction is given by

$$\hat{x}_{k+1}^{-} = F_k \hat{x}_k + G u_k \qquad (3\text{-}7)$$

the minus in the superscript of $\hat{x}$ denotes that the estimate has been made prior to taking a measurement.

The error covariance is also predicted during the prediction stage. The covariance matrix P is a $n \times n$ matrix representing the estimate error covariance. The covariance matrix is predicted via

$$P_{k+1}^{-} = F_k P_k F_k^T + Q_k \qquad (3\text{-}8)$$

b. Measurement

Once a prediction for the next state has been made, an actual measurement z_k is taken. Note once again that it is not necessary to measure every state being estimated. A quantity known as the residual $\tilde{z}_k$ is then calculated by

$$\tilde{z}_k = z_k - H_k \hat{x}_k^{-} \qquad (3\text{-}9)$$

A quantity called the Kalman gain is then defined according to

$$K_k = P_k^{-} H_k^T (H_k P_k^{-} H_k^T + R_k)^{-1} \qquad (3\text{-}10)$$

where

$$P_k = E[(x_k - \hat{x}_k)(x_k - \hat{x}_k)^T]$$
$$\text{and} \qquad (3\text{-}11)$$
$$\hat{x}_k^- = E[x_k \mid z_{k-1}]$$
$$\hat{x}_k^+ = E[x_k \mid z_k]$$

c. Correction

The Kalman gain in conjunction with the measurement residual are then used to find the estimate $\hat{x}_k$ via

$$\hat{x}_k = \hat{x}_k^- + K_K \tilde{z}_k \qquad (3\text{-}12)$$

The Kalman gain is also used to update the covariance matrix by

$$P_k^+ = (I - K_k H_k) P_k^- (I - K_k H_k))^T + K_k R_k K_k^T \qquad (3\text{-}13)$$

Once this has been completed, the process starts over again – hence the term recursive.

d. Filter Initialization

In order to begin the Kalman filtering process an initial estimate of both the state and the covariance matrix are required to begin the recursion. The filter can be initialized in several different ways, but the most common way to do so is via a simple guess. The closer to the actual state the initial guess is, the faster the estimate generated by the filter will reach the actual value. On occasion the filter is initialized using the first few measurements, but since it is easier to simply make an educated guess this method is not often used.

2. The Extended Kalman Filter

Not all processes that are desired to be estimated can be modeled in the linear form required for the Kalman filter. For these processes, the Extended Kalman Filter (EKF) can be used. The EKF is simply a regular Kalman filter that linearizes about the estimate and covariance.

For the EKF, the state vector *x* is governed by a non-linear function *f* dependent upon the current state, a control input, and plant noise

$$x_{k+1} = f(x_k, u_k, w_k) \qquad (3\text{-}14)$$

with the measurement z being expressed as a non-linear function of the state, as

$$z_k = h(x_k, v_k) \qquad (3\text{-}15)$$

Both noise terms w_k and v_k have the same properties as with the linear Kalman filter. Since it is impossible to know the noise at any given time and both the plant and measurement noise are characterized as white noise, both the state and measurement vectors are approximated by setting the noise equal to zero

$$\hat{x}_{k+1} = f(\hat{x}_k, u_k, 0) \qquad z_k = h(\hat{x}_k, 0) \qquad (3\text{-}16)$$

Linearizing about the zero mean non-linear functions in equation 3-16 will yield a close approximation to the actual value of the function itself – if the noise is truly zero-mean in nature, its expected value must be zero by definition. We linearize the system by taking the Jacobians of f and h with respect to the state vector x_k, and the following matrices are obtained

$$F_{i,j} = \frac{\partial f_i}{\partial x_j} \qquad (3\text{-}17)$$

$$H_{i,j} = \frac{\partial h_i}{\partial x_j} \qquad (3\text{-}18)$$

With the above matrices defined the EKF algorithm proceeds in exactly the same manner as the regular Kalman filter.

a. Prediction

The prediction for the EKF is done via the non-linear function f described previously. For the predicted state and covariance the equations are

$$\hat{x}_{k+1}^{-} = f(\hat{x}_k, u_k, 0) \qquad (3\text{-}19)$$

$$P_{k+1}^{-} = F_k P_k F_k^T + Q_k \qquad (3\text{-}20)$$

b. Measurement

Once a prediction has been made a measurement z_k is taken and as before, a residual $\tilde{z}_k$ is calculated, this time via the non-linear function *h*

$$\tilde{z}_k = z_k - h(\hat{x}_k^-, 0) \qquad (3\text{-}21)$$

The Kalman gain is calculated as before in equation 3-9, with the exception that when using the EKF *H* is the Jacobian of the non-linear function *h* vice the sensitivity matrix *H* used in the regular Kalman filter.

c. Correction and Initialization

As with the regular Kalman filter, the EKF corrects the estimate and the covariance matrix based upon the measurement and the Kalman gain. The equations used to do this are identical to the regular Kalman filter. Also like the regular Kalman filter, an EKF must be initialized with a starting value – like the correction step of the filtering process, the EKF method for initialization is identical to that used for the regular Kalman filter.

B. ATTITUDE ERROR REPRESENTATIONS

When using Kalman filters for spacecraft attitude estimation, the state vectors most frequently consist of bias and attitude errors. Prior to developing a Kalman filter for attitude estimation, it is appropriate to cover how the attitude error may be represented. The two attitude error representations relevant to the discussion here are the quaternion error and the Gibbs parameter error representations. Emphasis will be placed upon the latter of the two.

1. Quaternion Error

If two reference frames are slightly offset from one another, the error quaternion δq represents the rotation that will align one frame with the other. For example, if the estimated attitude of a spacecraft is given by q_{ref} and the measured attitude of the spacecraft by a perfect sensor was q then δq would represent the rotation from q_{ref}, the estimated attitude, to q, the actual attitude. For all rotations it can be shown that

$$q = \delta q \otimes q_{ref} \qquad (3\text{-}22)$$

The ease of processing the above equation makes the error quaternion a useful representation for spacecraft attitude error. However, from a Kalman filtering standpoint, the error quaternion presents some problems. Recall that when defining a residual, $\tilde{z}_k$ the estimated value is subtracted from the measured value. For illustrative purposes, define p as the measured error quaternion and q as the predicted error quaternion based upon the current state. Subtracting to obtain the residual yields

$$\tilde{z} = p - q = \begin{bmatrix} p_1 \\ p_2 \\ p_3 \\ p_4 \end{bmatrix} - \begin{bmatrix} q_1 \\ q_2 \\ q_3 \\ q_4 \end{bmatrix} = \begin{bmatrix} p_1 - q_1 \\ p_2 - q_2 \\ p_3 - q_3 \\ p_4 - q_4 \end{bmatrix} = \begin{bmatrix} \tilde{z}_1 \\ \tilde{z}_2 \\ \tilde{z}_3 \\ \tilde{z}_4 \end{bmatrix} \qquad (3\text{-}23)$$

While this seems straightforward enough, recall that attitude quaternions reside on the surface of a hyper-sphere defined previously and shown again here

$$q_1^2 + q_2^2 + q_3^2 + q_4^2 = 1 \qquad (2\text{-}5)$$

Though p and q both satisfy the requirements of equation 2-5 their difference will not do so, and therefore is not an attitude quaternion. This becomes a problem when using quaternions in a Kalman filtering algorithm, so converting the quaternion to different representations becomes necessary – as will be shown later in this chapter.

2. Gibbs Error

Although the Gibbs parameter is closely related to the quaternion – as one can easily see from its definition in chapter two – it does not have the normalization constraint. The Gibbs parameter for a particular quaternion resides in a plane tangent to the surface of the hyper-sphere on which quaternions reside. A direct mapping between the Gibbs parameter plane and the quaternion hyper-sphere exists and is given by

$$\delta q(a_g) = (4 + a_g)^{-\frac{1}{2}} \begin{bmatrix} a_g \\ 2 \end{bmatrix} \qquad (3\text{-}24)$$

It can further be shown that the direction cosine matrix associated with a particular $\delta q(a)$ may be approximated by

$$A(\delta q(a)) \approx I_{3\times 3} - [a\times] - \frac{1}{2}(a^2 I_{3\times 3} - aa^T) \qquad (3\text{-}25)$$

This direct relationship between the Gibbs parameter and the quaternion will be used in the next section to formulate a Kalman filter for spacecraft attitude estimation [Markley].

C. FORMULATION OF A GIBBS PARAMETER BASED KALMAN FILTER

With the Kalman filter and attitude error representation introduced, the formulation of the Kalman filter may be developed. The Kalman filter developed in this section estimates the spacecraft attitude error and the gyroscopic bias. It uses a six element state vector of the form

$$x = \begin{bmatrix} a(t) \\ b(t) \end{bmatrix} \qquad (3\text{-}26)$$

where *a(t)* represents the attitude error in Gibbs parameters and *b(t)* is the gyroscopic bias error.

1. Filter Overview

The Kalman filter developed here is based on one developed by F. Landis Markley [Markley]. It treats the actual attitude as the quaternion product of the estimated quaternion error and the previous estimate, as shown here

$$q(t) = \delta q(a(t)) \otimes q_{ref} \qquad (3\text{-}27)$$

where q_{ref} is the attitude estimate from the previous time step and $\delta q(a(t))$ represents the rotation from the last time step to the attitude at the current time step.

The steps for the filter are the same as for any other – prediction, measurement update, and correction. What is unique about this filter is that the propagation of the state vector $x = \begin{bmatrix} a(t) \\ b(t) \end{bmatrix}$ is relatively trivial in nature, as Markley himself states. Prior to developing the filter itself, it is of interest to show why this is the case.

In the prediction step of this filter, the attitude quaternion from the previous time step q_{ref}^{-} is considered the optimal estimate for the attitude of the spacecraft, i.e. the attitude error estimate $\hat{a}^{-}(t)$ at the beginning of every time step is zero by definition. Once a measurement is taken, q_{ref}^{-} is no longer the optimal estimate for the spacecraft

attitude. During the correction step, the corrected error estimate $\hat{a}^{+}(t)$ is used to propagate the old estimate, q_{ref}^{-} so that it becomes the new optimal estimate for the spacecraft attitude via

$$q_{ref}^{+} = \delta q(\hat{a}^{+}(t)) \otimes q_{ref}^{-} \qquad (3\text{-}28)$$

Once the new optimal estimate has been generated, $\hat{a}(t)$ is immediately reset to zero. When the next step in the recursion begins, the new q_{ref}^{-} then becomes the optimal estimate

$$q_{ref}^{-} = \delta q(\hat{a}^{-}(t)) \otimes q_{ref}^{-} = \delta q(0) \otimes q_{ref}^{-} = q_{ref}^{-} \qquad (3\text{-}29)$$

Because the filter is designed in this manner, the actual propagation of the state vector is trivial because its first three elements are always reset to zero. The value of q_{ref}^{-} immediately after the correction step of the filtering process is the actual attitude estimate – the state vector merely tracks the error.

2. System Dynamics – Developing the State Transition Matrix

The first step in formulating any Kalman filter is mathematically modeling how the system should behave and subsequently constructing a state transition matrix based upon this mathematical model. For a satellite, we have its current state quaternion and its angular rate ω. From equation 2-12, it is known that the time derivative of the quaternion is based upon the angular rate of the body it is describing.

Placing this in terms of the filter formulation

$$\dot{q}_{ref} = \frac{1}{2}\begin{bmatrix} \vec{\omega}_{ref} \\ 0 \end{bmatrix} \otimes q_{ref} \qquad (3\text{-}30)$$

where $\vec{\omega}_{ref}$ is the angular rate of the satellite at the reference attitude, q_{ref}.

The filter itself is not estimating the quaternion components of the attitude – it estimates the error in terms of Gibbs parameters. The equation for the propagation of the Gibbs parameter error is given by

$$\dot{a}_g = (I_{3\times 3} + \frac{1}{4} a_g a_g^T)(\omega - \omega_{ref}) - \frac{1}{2}(\omega + \omega_{ref}) \times a_g \equiv f(a,t) \qquad (3\text{-}31)$$

as shown by Markley [Markley].

We now propagate the estimate from time nT to time $nT+T$. Therefore

$$q_{ref} = q(nT) = \text{constant} \qquad (3\text{-}32)$$

and $\omega_{ref} = 0$ since q_{ref} is constant. Therefore, from equation 3-27 we obtain

$$q(nT+T) = \delta q(a(nT+T)) \otimes q(nT) \qquad (3\text{-}33)$$

Propagating in a discrete manner, $a_g(nT+T)$ may be written as

$$a_g(nT+T) = a_g(nT) + \dot{a}_g T \qquad (3\text{-}34)$$

When this approach is taken, equation 3-31 may be rewritten as

$$\dot{a}_g = (I_{3\times 3} + \frac{1}{4} a_g a_g^T)\omega - \frac{1}{2}\omega \times a_g \qquad (3\text{-}35)$$

Linearizing about a_g yields the following equation

$$\dot{a}_g = \omega - \frac{1}{2}\omega \times a_g \qquad (3\text{-}36)$$

Recalling from equation 2-16 that the angular velocity is actually a function of the measured velocity and the gyroscopic bias and substituting that into equation 3-36 (assuming a zero noise component for the time being) gives

$$\begin{aligned} \dot{a}_g &= \omega_{meas} - b - \frac{1}{2}(\omega_m - b) \times a_g \\ &\simeq \omega_{meas} - b - \frac{1}{2}\Omega_m a_g \end{aligned} \qquad (3\text{-}37)$$

Introducing the term Ω_m which is defined as the skew of the measured angular velocity

$$\Omega_m = [\omega_{meas} \times] = \begin{bmatrix} 0 & -\omega_{meas_z} & \omega_{meas_y} \\ \omega_{meas_z} & 0 & -\omega_{meas_x} \\ -\omega_{meas_y} & \omega_{meas_x} & 0 \end{bmatrix} \qquad (3\text{-}38)$$

We propagate the attitude from time nT to time $nT+T$ equation 3-34 may be rewritten as

$$\begin{aligned} a_g(nT+T) &= a(nT) + (\omega_{meas}(nT) - b(nT) - \frac{1}{2}\Omega_m(nT)a(nT))T \\ &= (I_{3\times3} - \frac{1}{2}\Omega_m(nT)T)a(nT) + \omega_{meas}(nT)T - b(nT)T \end{aligned} \tag{3-39}$$

Assuming a constant bias over short periods of time T, the state equation 3-39 may be used to formulate the state transition matrix for the Kalman filter

$$A_d = \begin{bmatrix} I_{3\times3} - \frac{1}{2}\Omega_m T & -I_{3\times3}T \\ \varnothing_{3\times3} & I_{3\times3} \end{bmatrix} \tag{3-40}$$

which will propagate the state as

$$x(nT+T) = A_d x(nT) + u(nT) + w(nT) \tag{3-41}$$

This is in the standard state space form so we are able to apply standard Kalman filtering algorithms with the control input modeled as

$$u = \omega T \tag{3-42}$$

3. System Sensors - Developing the Measurement Sensitivity Matrix

With the state transition matrix developed from the system dynamics, it becomes necessary to determine how the filter will take an external measurement and incorporate it into the filtering algorithm via the measurement sensitivity matrix. The term which drives the 'correction' equation is the error between the actual measurement and the predicted measurement. In particular in our problem we have the actual orientation ${}^{i}v$ from the star trackers library in the inertial coordinate frame. At the same time, given an estimate of the spacecraft orientation $\hat{q}$ and the observed star ${}^{b}v$ from the star tracker we can compute and estimate

$${}^{i}\hat{v} = A(\hat{q})\,{}^{b}v \tag{3-43}$$

In particular let

$$\hat{q} = \delta q(a) \otimes q^{+}(nT) \tag{3-44}$$

so the error ${}^{i}v - {}^{i}\hat{v}$ can be written as

$$ {}^{i}v - {}^{i}\hat{v} = {}^{i}v - A(\delta q(a))A(\hat{q}^{+}(nT)){}^{b}v \qquad (3\text{-}45) $$

Substituting equation 3-35 into the above equation produces a relationship between the Gibbs error a, q_{ref}, ${}^{b}\vec{v}$ and ${}^{i}\vec{v}$

$$ {}^{b}\vec{v} = [I_{3\times3} - [a\times] - \frac{1}{2}(a^2 I_{3\times3} - aa^T)]A(q_{ref}){}^{i}\vec{v} \qquad (3\text{-}46) $$

In the above equation q_{ref} is the estimate from the previous time step. Conducting a first order expansion with respect to the Gibbs error about ${}^{b}\vec{\vec{v}}$ yields the following equation

$$ h({}^{b}\vec{v}) = h({}^{b}\vec{\vec{v}}) + \left.\frac{\partial h}{\partial {}^{b}\vec{v}}\right|_{{}^{b}\vec{\vec{v}}} [a\times]{}^{b}\vec{\vec{v}} = h({}^{b}\vec{\vec{v}}) + H_a a \qquad (3\text{-}47) $$

From this, H_a is shown to be

$$ H_a \equiv \left.\frac{\partial h}{\partial {}^{b}\vec{v}}\right|_{{}^{b}\vec{\vec{v}}} [{}^{b}\vec{\vec{v}}\times] \qquad (3\text{-}48) $$

With the above relations developed, the measurement sensitivity matrix can be formed by relating them to the state vector x

$$ H = [H_a \ \varnothing_{3\times3}] \qquad (3\text{-}49) $$

4. The Filter Equations

With the state transition and measurement sensitivity equations constructed, it is now possible to summarize and implement the Kalman filter. In this version of the filter, the prediction and correction steps are combined for expediency.

The Kalman filter is built on the following state space model, developed above

$$ \begin{aligned} x(n+1) &= \begin{bmatrix} -\frac{1}{2}\Omega_m & -I_{3\times3} \\ \varnothing_{3\times3} & \varnothing_{3\times3} \end{bmatrix} x(n) + \begin{bmatrix} u \\ 0_{1\times3} \end{bmatrix} + w = Ax + Bu + w \\ y(n) &= \left[\left.\frac{\partial h}{\partial {}^{b}\vec{v}}\right|_{{}^{b}\vec{\vec{v}}} [{}^{b}\vec{\vec{v}}\times] \ \varnothing_{3\times3} \right] x(n) + v = Hx + v \end{aligned} \qquad (3\text{-}50) $$

where $x(n) = \begin{bmatrix} a \\ b \end{bmatrix}$ and $u(n) = \omega_{meas} T$.

The following equations are used to estimate the state and the covariance

$$\hat{x}_{k+1} = \begin{bmatrix} I_{3\times3} - \frac{1}{2}\Omega_m T & -I_{3\times3} T \\ \varnothing_{3\times3} & I_{3\times3} \end{bmatrix} \hat{x}_k + K(z_k - [[{}^b\vec{\tilde{v}}\times] \varnothing_{3\times3}]\hat{x}_k) + u$$

$$= A_d \hat{x}_k + K(z_k - H\hat{x}_k) + u \tag{3-51}$$

$$P_{k+1} = A_d P_k A_d^T + Q - K_k (H P_k H^T + R) K_k{}^T \tag{3-52}$$

Note that the above two equations differ slightly from the Kalman filtering equations derived earlier. For implementation purposes, the prediction and correction steps were combined. It is also important to note here that the measurement z_k is the measured error, which is given by

$$z_k = {}^b\vec{\tilde{v}} - {}^b\vec{v} \tag{3-53}$$

The Kalman gain *K* used in equation 3-60 is calculated by

$$K_k = A_d P_k H^T (H P_k H^T + R)^{-1} \tag{3-54}$$

A diagram of the filtering process is shown in Figure 4. The reference quaternion which is updated after the filter estimates the attitude error gives the optimal estimate of the attitude of the spacecraft after it is updated with the information from the filter. Once the reference quaternion becomes the optimal estimate, the attitude error estimate is reset to zero.

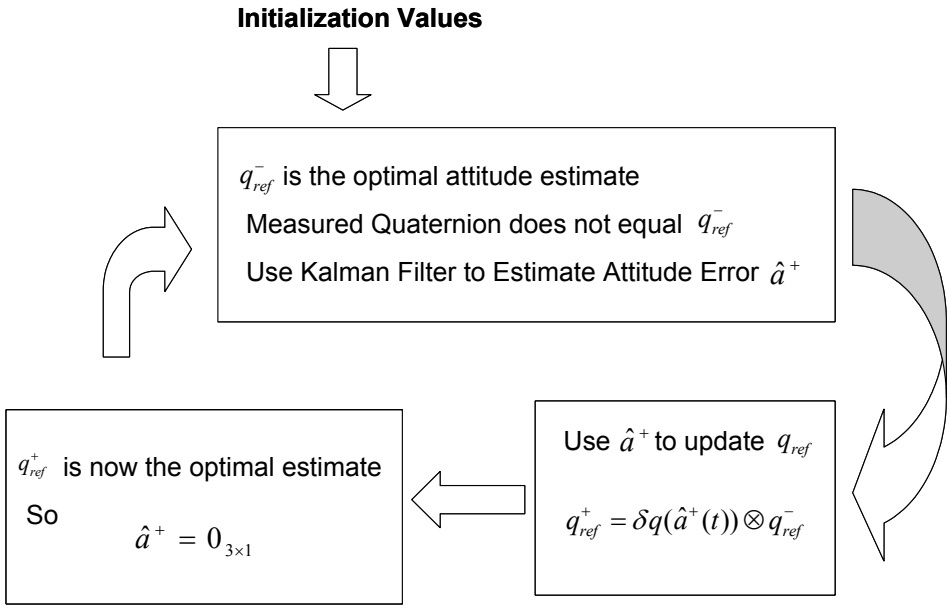

Figure 4. Gibbs Parameter Kalman Filter Flow Diagram

5. Testing the Filter

Once developed, the filter was implemented in MATLAB and tested using both 'clean' and corrupted quaternion measurements taken from a simulated satellite that drives itself to nadir pointing after an initial offset. The gyroscopes in this simulation had no bias. Clean quaternions and gyroscope readings were used on this initial run to see if the Kalman filter would function correctly. The results are shown in figures five and six. Though some quaternion error is present, it is on the order of 10^{-6} and is attributed to numerical error only. The estimated bias is of the same order and is also attributed to numerical errors and the fact that a non-zero value for the bias was used to initialize the filter. Because of the low level of error, it was concluded that the filter functions correctly.

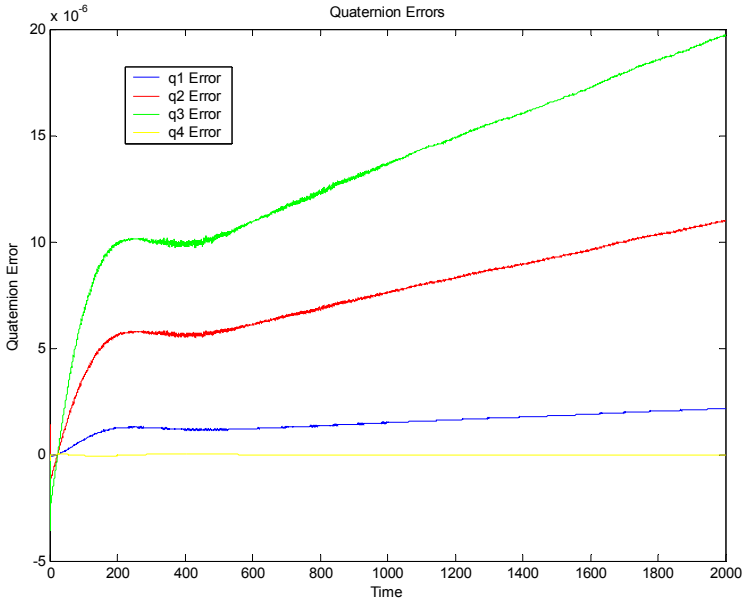

Figure 5. Quaternion Errors For Gibbs Parameter Kalman Filter With Zero Bias and No Measurement Noise

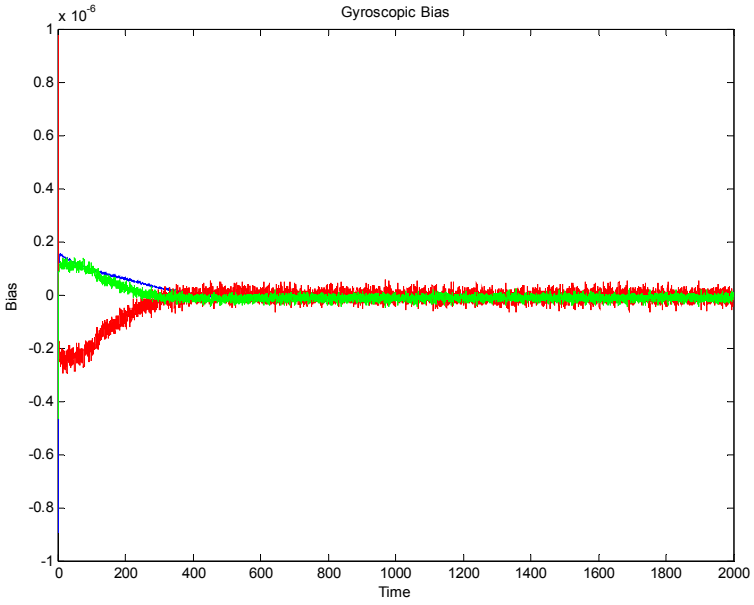

Figure 6. Bias Estimated By Gibbs Parameter Kalman Filter with Zero Bias and No Measurement Noise

THIS PAGE INTENTIONALLY LEFT BLANK

IV. STAR GAP ERROR MITIGATION

As a satellite travels in its orbit about the Earth, there will be times when none of its star trackers are able to feed an attitude quaternion into the attitude control system. There are several possible reasons for these star gaps, including solar and lunar entry into the field of view (FOV) of the star tracker, processing time for the tracker to find and lock on a new star(s) once the previous one(s) exit the FOV, or due to a reorientation maneuver by the satellite – among others. These gaps have marked effects upon attitude estimation algorithms. In this section the effects of star gaps are examined – both for the Gibbs parameter based Kalman filter developed in Chapter Three and an Euler angle based Kalman filter developed by Palermo using the same data [Palermo]. Methods to mitigate the effects of these star gaps are presented along with simulated results of their implementation.

A. EFFECTS OF STAR GAPS

When a star gap occurs, the effect it has on the attitude estimation algorithm is highly dependent upon the formation of that algorithm. Regardless of the type of algorithm in use, a longer star gap equates to a larger error as will be shown in the results later in this section.

1. Euler Angle Based Kalman Filter

Prior to examining how star gaps affect the Euler angle based Kalman filter it is useful to briefly examine its formulation. For a full derivation of the equations, the reader is referred to [Palermo]. When a star gap occurs in the Euler angle based Kalman filter, the attitude estimate diverges for all four elements of the quaternion. Upon reacquisition of a star, there is a brief spike in the attitude error then the measurement updates drive the error back down – eventually. The results of a 200 second star gap on an attitude estimator based upon Euler angles are shown in the following figure. The estimator is tracking noisy measurements for both attitude and angular rate.

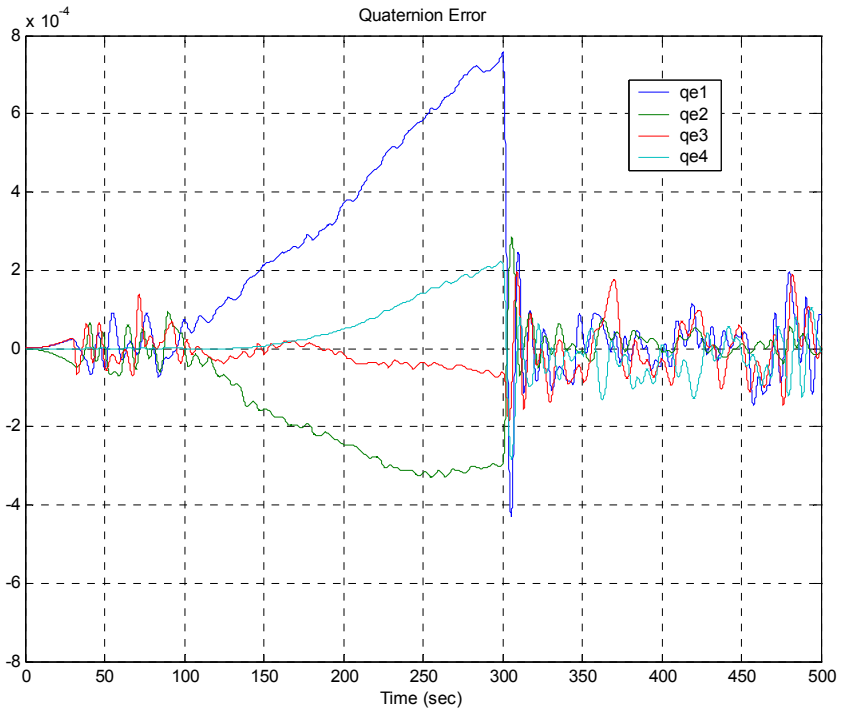

Figure 7. Euler Angle Based Kalman Filter with 200 Second Star Gap

2. Gibbs Parameter Based Kalman Filter

The Gibbs Parameter based Kalman Filter behaves in a very different manner. When a star gap occurs, the estimator is able to continue the track with excellent accuracy because it is still receiving angular rate data. The measured angular rate data allows the estimator to propagate the reference quaternion q_{ref} with little loss of accuracy due to the star gap. The graph was made using the exact same data for a 200 second star gap as was used for the Euler angle based Kalman filter. Figure 8 shows the quaternion errors for the same track.

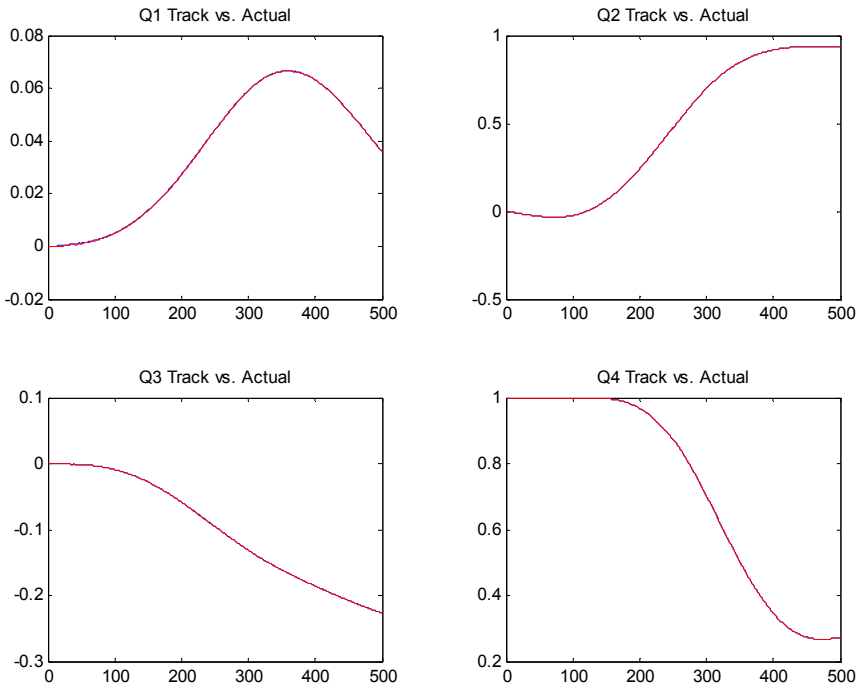

Figure 8. Estimated Quaternion Elements vs. Actual for Gibbs Parameter Based Kalman Filter (Estimate Shown in Blue) with 200 Second Star Gap

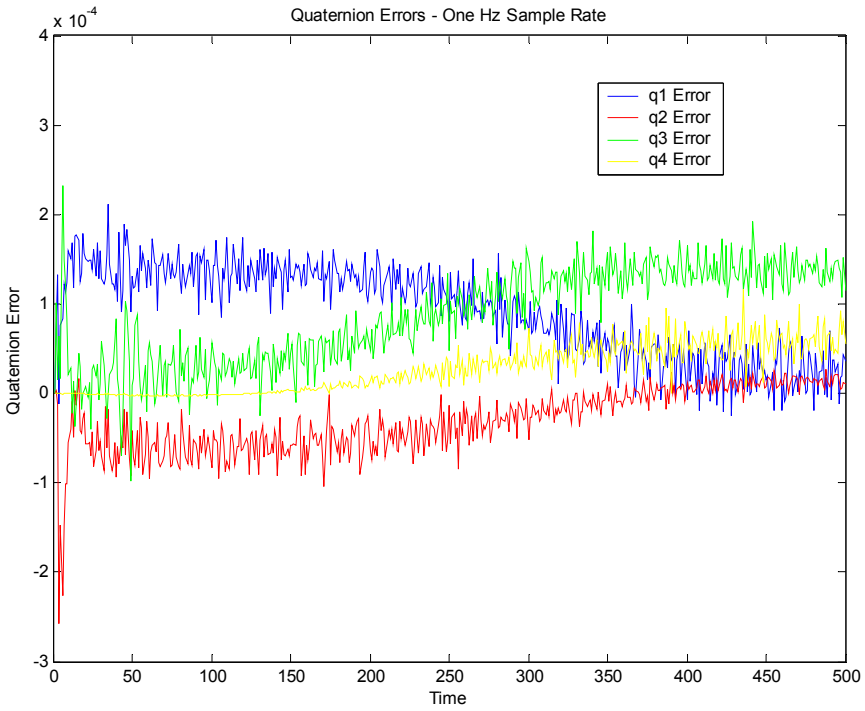

Figure 9. Quaternion Error for Gibbs Parameter Based Kalman Filter with 200 Second Star Gap

B. ADAPTIVE COVARIANCE

One technique for mitigating the effects of a star gap is adapting the different covariance matrices intrinsic to the Kalman filtering process. The three matrices dealing with covariance are the filter covariance matrix P, the plant covariance matrix Q, and the measurement covariance matrix R. The P matrix is predicted and corrected based upon measured values and the Kalman gain – adapting it based upon situational parameters would significantly change the way in which the filter propagates the estimate. The plant and measurement covariance matrices, however, remain constant throughout the filtering process. The performance of any Kalman filter may be modified by changing their value. By doing so adaptively based upon external conditions, it is possible to mitigate some of the attitude error caused by intermittent star gaps. Adaptation of the plant and measurement covariance are examined individually and then examined in conjunction with one another.

C. THE PLANT COVARIANCE MATRIX

The plant covariance Q may be thought of as a measure of how well the model emulates the actual dynamics of the quantities being estimated. The more precise the model, the lower the values contained in the Q matrix. A star gap might be conceptualized as a system modeled in an extremely poor manner, i.e. a system with an extremely large plant noise. Using this conceptualization, a trigger was developed that increased the plant covariance when a star gap occurred. This covariance trigger was implemented on both the Euler and Gibbs parameter based Kalman Filters.

1. Adapting Plant Noise for the Euler Angle Based Kalman Filter

The Euler angle based Kalman Filter used for testing the adaptive covariance concept was developed by Palermo using SIMULINK [Palermo]. This format was maintained, but modified to adapt the covariance matrices. The following figure shows the trigger that was developed for this purpose. The figure shown is the measurement covariance trigger – the plant noise covariance trigger is identical. An initial matrix serves as the covariance trigger until a certain point – user determined – at which it is increased by a user determined factor. After a certain time period has elapsed, the covariance matrix is reset to its initial value. A digital clock was used to do this, as can be seen in the diagram.

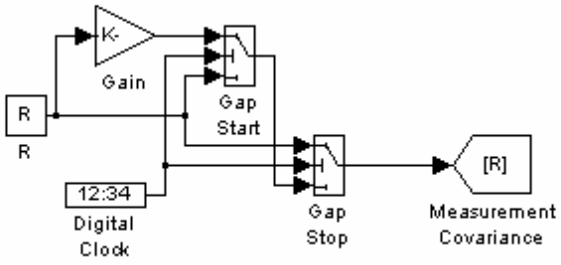

Figure 10. Measurement Covariance Trigger

Once the covariance trigger was implemented, it was tested using several different gains for the 200 second star gap under consideration. Note that the trigger was timed to increase the covariance just before the star gap and decrease it immediately just after the star gap – assuming that the measurements preceding the star gap were stored in memory and recycled through with the new value of Q once the star gap was detected. Both the magnitude and the directions of the rotations varied for each gain used. The gains for the plant noise covariance matrix were increased logarithmically for the duration of the star gap. The following figures shows the mean quaternion errors plotted against the gains applied to the plant noise matrix Q for the duration of the star gap.

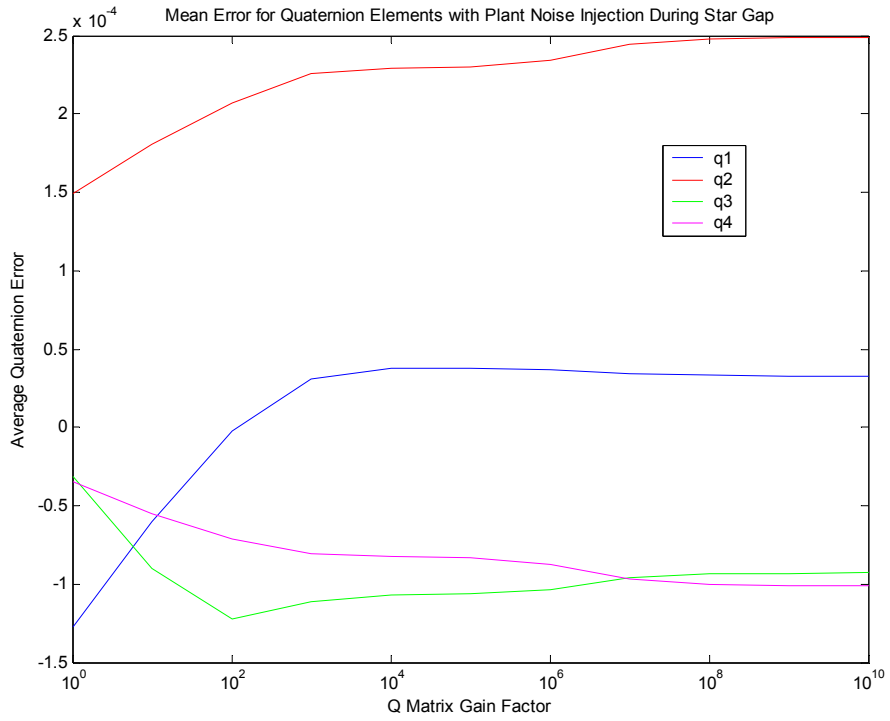

Figure 11. Mean Quaternion Error for Plant Noise Injection During Star Gaps

2. Adapting Plant Noise for the Gibbs Parameter Based Kalman Filter

The Kalman filter based on Gibbs Parameters was built in MATLAB without using SIMULINK, making any adaptation of the Q matrix easy to accomplish. Unlike the Euler angle based Kalman filter, adapting the plant noise with the Gibbs Parameter based Kalman filter produced no noticeable effect.

D. THE MEASUREMENT COVARIANCE MATRIX

The measurement covariance matrix R provides the filter with the known accuracies of the sensors being used to take the measurements z. Conceptually, it follows that when a sensor is producing no measurement its function should come into question. This was done for both types of Kalman filters discussed in this paper.

1. Perturbation of Measurement Noise Covariance Matrix for an Euler Angle Based Kalman Filter

Adapting the measurement covariance matrix accordingly using the trigger shown in figure eight produced the following results when applied to the Euler angle based Kalman filter.

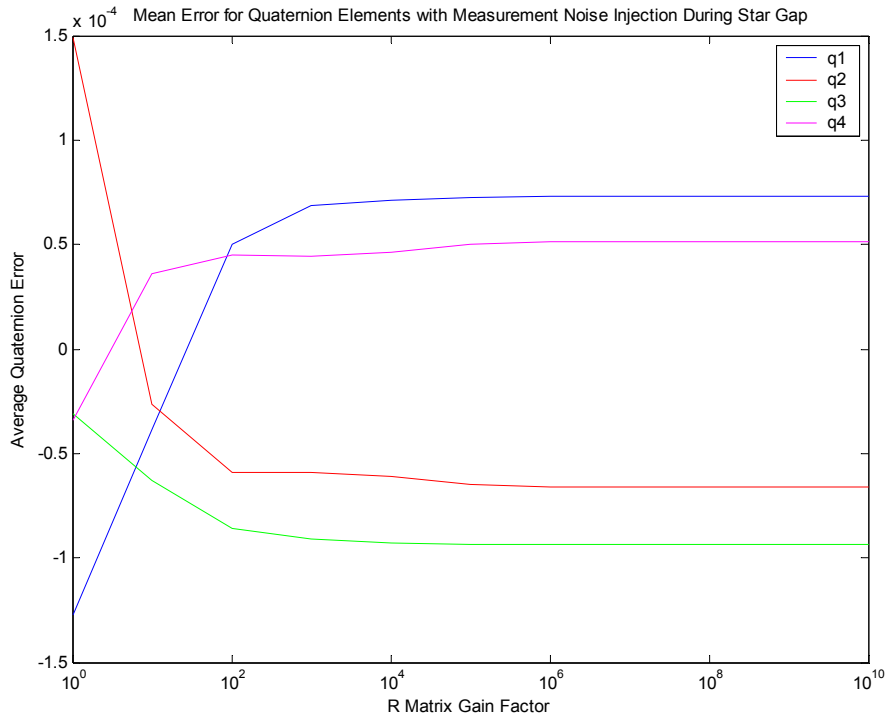

Figure 12. Mean Quaternion Error for Measurement Matrix Adaptation During Star Gap

2. Perturbation of Measurement Noise Covariance Matrix for a Gibbs Parameter Based Kalman Filter

As with the plant noise injection, measurement noise injection for the Gibbs parameter based Kalman filter produced no difference with regards to estimation error encountered during a star gap.

E. SIMULTANEOUS ADAPTATION OF COVARIANCE MATRICES

If adjusting the sensitivity of the filter to plant and measurement noise individually affects the average quaternion error for a Kalman filter, it follows that adapting both simultaneously would do so as well. This was accomplished via use of two triggers operating in parallel, as shown previously in figure eight. The results are shown in the following figure – a significant improvement over adapting either matrix individually.

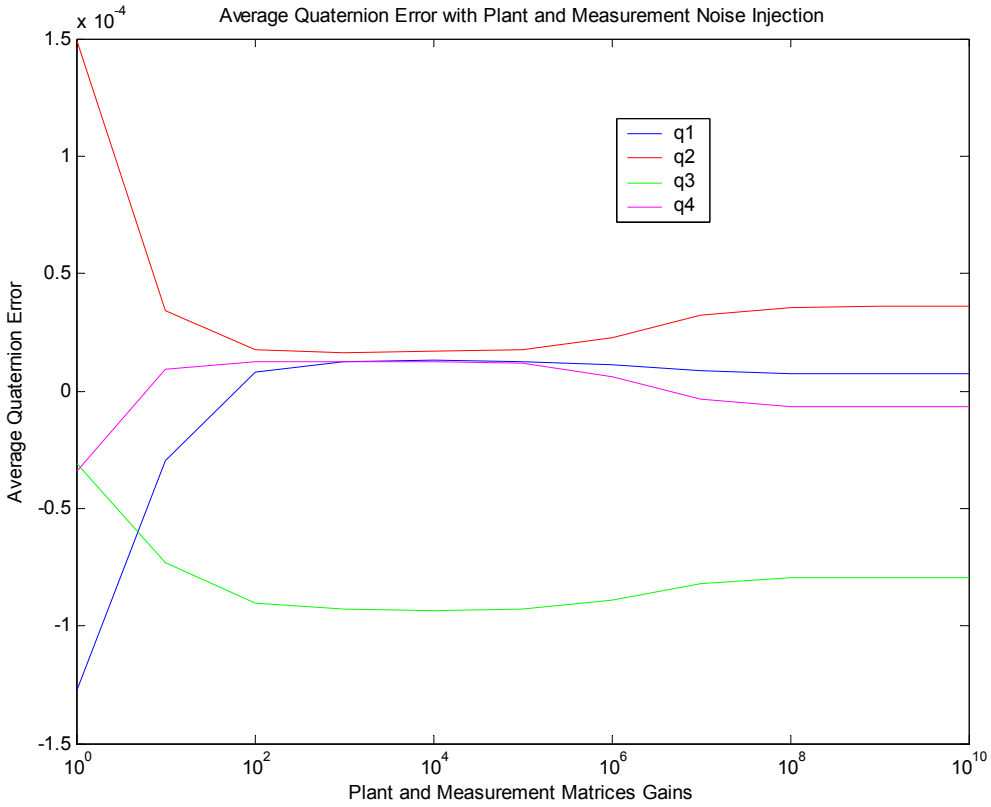

Figure 13. Average Quaternion Error with Simultaneous Plant and Measurement Covariance Matrix Adaptation

Adaptation of the plant noise and measurement noise matrices is an option for mitigating attitude estimation error in some cases, as has been shown in the preceding sections. While it does not eliminate the error induced due to star gaps, it does have the potential to reduce the amount of error encountered.

V. DYNAMIC GYROSCOPE AND RATE GYRO UPSETS

Mechanical rate gyroscopes have historically been a weak point in satellite design. Their high failure rate coupled with their noisy output and importance in attitude estimation makes them a liability from a reliability standpoint. Improved gyroscopes have been developed – such as the laser gyroscope – but many systems currently in orbit are still relying on mechanical gyroscopes which are both noisy and prone to failure. This chapter introduces the dynamic gyroscope – a software alternative to the rate gyroscope, shows how rate gyroscope upsets can affect attitude estimation algorithms, and then integrates the dynamic gyroscope with attitude estimation algorithms to mitigate the effects of rate gyroscope upsets.

A. THE RATE GYROSCOPE UPSET

The rate gyroscope upset is a phenomenon that has been occurring on certain satellites in orbit. At certain random points in time the rate gyroscope will send a measurement to the attitude control system that is 100 to 1000 times the actual reading. This wreaks havoc on the control system, as can be seen in the following two figures. Both figures were produced with the same data from a simulated satellite – with a simulated rate gyroscope upset. The simulated rate gyroscope upset was of two seconds duration with a measurement 1000 times the correct reading being sent to the attitude estimation system. As can be seen by looking at the figures, the Gibbs Parameter based Kalman Filter developed earlier performs extremely well as compared to the Euler angle based filter. After a brief jump in estimator error, the attitude error for the Gibbs Parameter Kalman filter returns to the order of 10^{-4} while the Euler Angle Kalman filter is unable to recover any semblance of accuracy after an upset occurs.

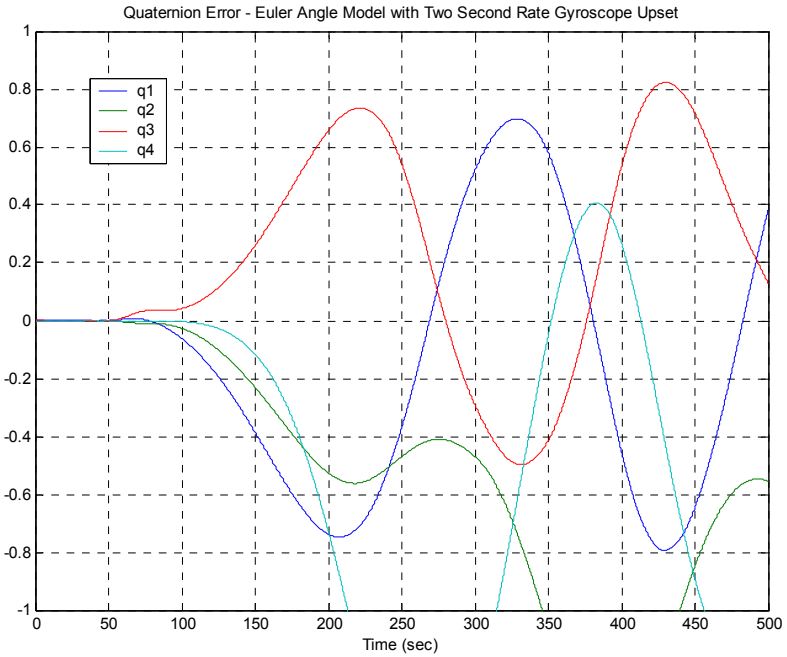

Figure 14. Quaternion Error with 2 second Rate Gyroscope Upset – Euler Angle Based Kalman Filter

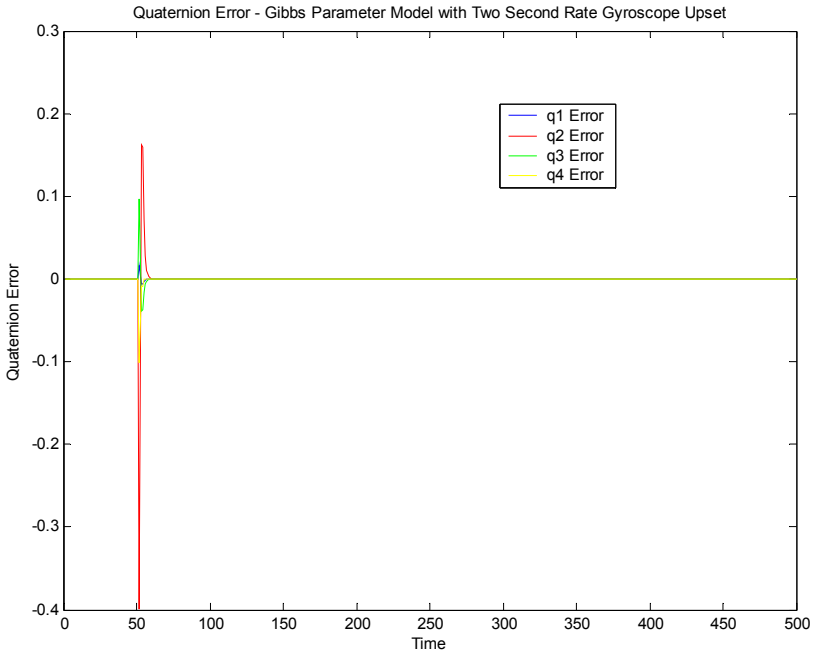

Figure 15. Quaternion Error with 2 second Rate Gyroscope Upset – Gibbs Parameter Based Kalman Filter

Rate gyroscope upsets of longer and longer lengths were tested on the Gibbs Parameter Kalman filter, as shown in figure 16 and up to a certain point the attitude estimator was able to recover its pre-upset estimation accuracy. After a certain time period the estimator does lose its ability to recover from an upset, as shown in figure 17 when the rate gyroscope upset was 150 seconds in length. However, its superiority over the Euler Angle Kalman filter remains apparent.

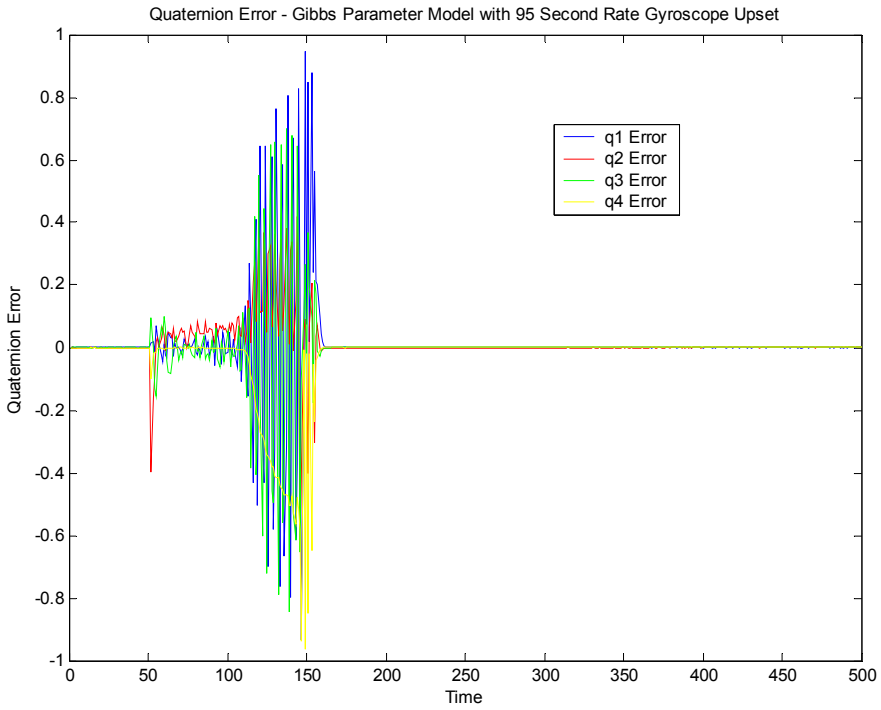

Figure 16. Gibbs Parameter Based Kalman Filter with 95 second Rate Gyroscope Upset

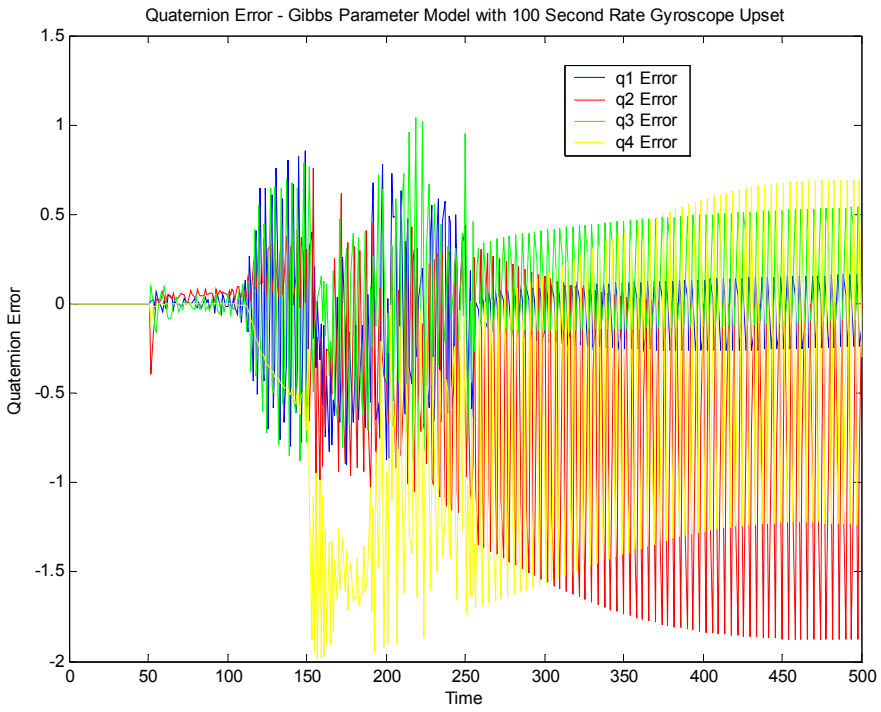

Figure 17. Gibbs Parameter Based Kalman Filter with a 150 Second Rate Gyroscope Upset

A bit of analysis revealed that the covariance matrix for the Kalman Filter was positive semi-definite for all in which it was able to recover from the rate gyroscope upset. If the covariance matrix became non-positive semi-definite during the rate gyroscope upset, the filter would not recover.

B. THE DYNAMIC GYROSCOPE

It is possible to mathematically model and predict all of the external torques on a satellite with some degree of accuracy – some more than others. Recall from basic physics that the torque N of a satellite during a time period may be expressed as

$$N_{satellite} = \int_{t_k}^{t_{k+1}} \dot{\vec{H}} dt \qquad (5\text{-}1)$$

Equation 5-1 may further be broken down because the torques on a satellite may be expressed as the sum of its external torques – which may be mathematically modeled – and its internal torques from any momentum exchange devices. Equation 5-1 may therefore be written as

$$\vec{N}_{satellite} = \vec{N}_{ext} + \vec{N}_{MED} = \int_{t_k}^{t_{k+1}} \dot{\vec{H}} dt \qquad (5\text{-}2)$$

It follows that

$$\vec{N}_{ext} + \vec{N}_{MED} = \int_{t_k}^{t_{k+1}} \dot{\vec{H}} dt = \vec{H}_{t_{k+1}} - \vec{H}_{t_k} \qquad (5\text{-}3)$$

Assuming that any change in the moment of inertia between t_{k+1} and t_k will be negligible and recalling that

$$\vec{H}_k = I\vec{\omega}_k \qquad (5\text{-}4)$$

It follows that

$$\begin{aligned} \vec{H}_{t_{k+1}} - \vec{H}_{t_k} &= I(\vec{\omega}_{k+1} - \vec{\omega}_k) \\ \vec{\omega}_{k+1} - \vec{\omega}_k &= I^{-1}(\vec{H}_{t_{k+1}} - \vec{H}_{t_k}) \\ \vec{\omega}_{k+1} &= \vec{\omega}_k + I^{-1}(\vec{H}_{t_{k+1}} - \vec{H}_{t_k}) \end{aligned} \qquad (5\text{-}5)$$

Inserting equation 5-3 into equation 5-5 gives a way to predict the angular momentum for t_{k+1} given only known or mathematically modeled data

$$\vec{\omega}_{k+1} = \vec{\omega}_k + I^{-1}(\vec{N}_{ext} + \vec{N}_{MED}) \qquad (5\text{-}6)$$

Using equation 5-6 or some variant thereof, the angular momentum of a satellite may be obtained analytically. An algorithm that calculates the angular rate in this manner is referred to as a dynamic or a pseudo-gyroscope. Such a gyroscope was developed by Aerospace Corporation and a variant of this was implemented by Palermo [Palermo]. The following figure shows a comparison of a simulated real gyroscope and the Palermo dynamic gyroscope. The dynamic gyroscope produces a reading very close to that produced by the real gyroscope. While rate error is not absent, the amount of error – shown in figure 19 – is such that the resulting attitude error will be manageable.

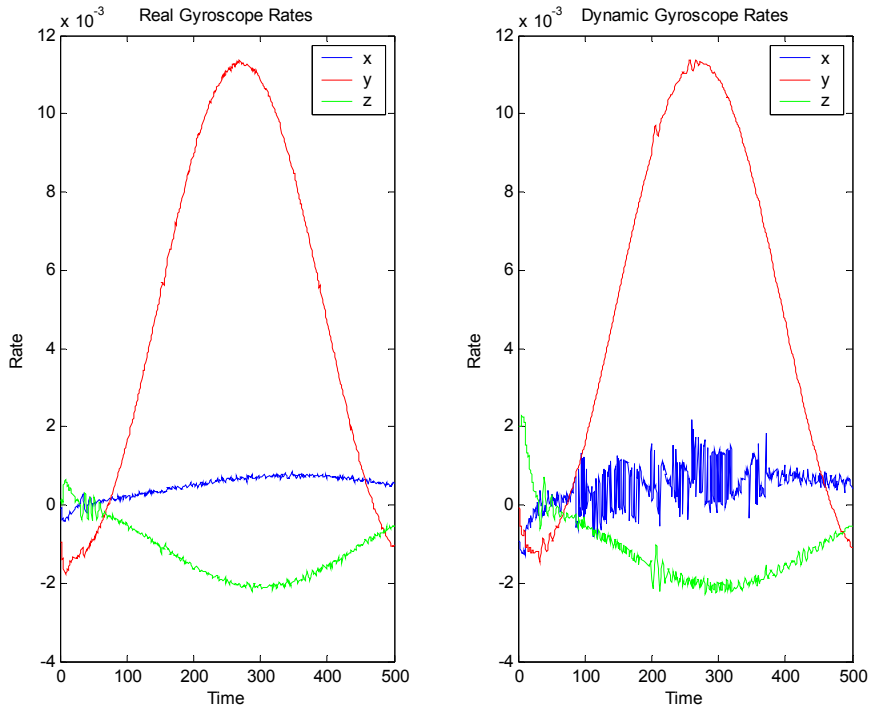

Figure 18. Comparison of Real and Dynamic Gyroscope Performance

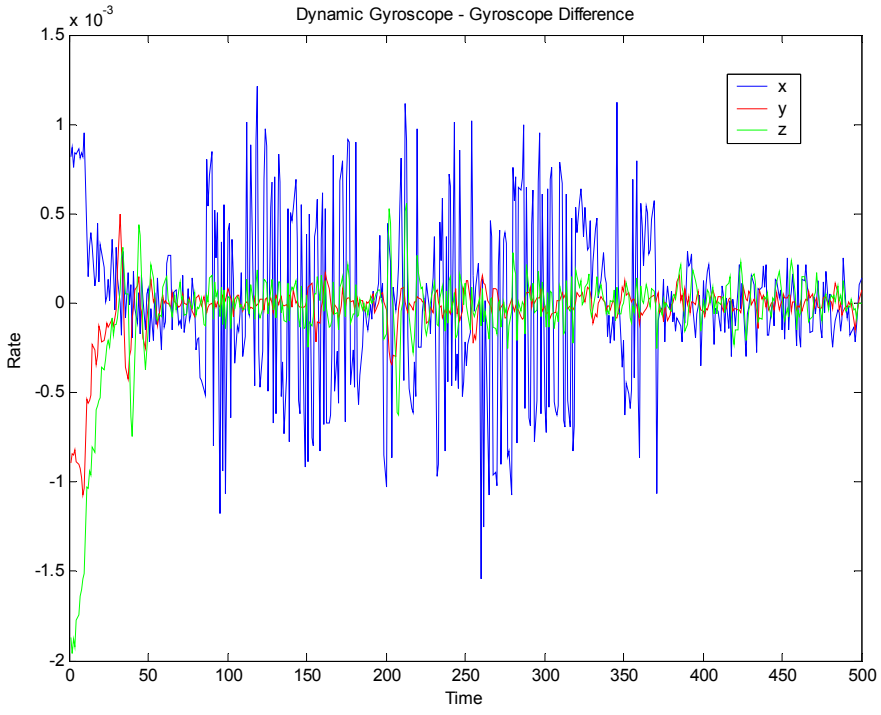

Figure 19. Difference Between Real and Dynamic Gyroscope Readings

Though convenient, dynamic gyroscopes are not free of problems. Any inaccuracy in knowledge of the moment of inertia of the spacecraft will result in angular rate errors, as can be seen from equation 5-6. Any expenditure of fuel, movement of fuel due to any slew maneuver or satellite motion, or any movement of the solar arrays – among other things – will change the moment of inertia of a satellite, thereby causing some error. System identification algorithms can be used to help mitigate this problem, but such algorithms are not perfect – error will always remain.

C. INTEGRATING THE DYNAMIC GYROSCOPE WITH AN ATTITUDE ESTIMATOR

By using a dynamic gyroscope in conjunction with a real mechanical gyroscope it is possible to mitigate the effect of a rate-gyroscope upset. As seen in the above figures, the dynamic gyroscope is able to produce data quite close to that of a real gyroscope. Given the fact that the Gibbs Parameter based Kalman filter is extremely robust with regards to recovering from rate gyroscope upsets and the fact that any mechanism for switching from regular gyroscope readings to measurements from the dynamic gyroscope will be imperfect, the Gibbs Parameter based Kalman filter is an ideal estimator with which to integrate the dynamic gyroscope. The following figure shows the quaternion error for a Gibbs parameter based Kalman filter with a 95 second rate gyroscope upset of 1000 times the actual reading. The dynamic gyroscope in this scenario took over immediately so no upset readings entered the estimator.

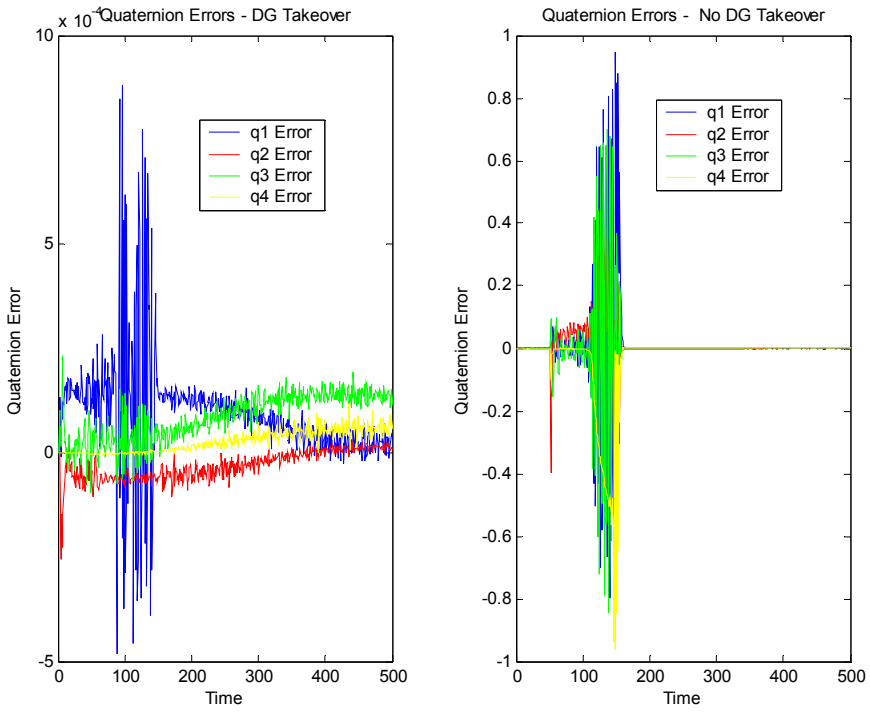

Figure 20. Comparison of Estimator Performance with and without Dynamic Gyroscope input during a 95 second Rate Gyroscope Upset

As can be seen, when a dynamic gyroscope is in use and no data from the real gyroscope during its upset period reaches the estimator, the amount of error encountered is only slightly increased. As mentioned earlier, this would be an ideal scenario. It would be impossible to design a perfect algorithm where the dynamic gyroscope data would replace the real gyroscope measurements immediately. Some upset data would always have a chance of getting into the estimator. The robustness of the Gibbs parameter based Kalman filter to short rate gyroscope upsets was shown previously. The following figure shows a scenario in which the dynamic gyroscope takes over two measurements after the commencement of the rate gyroscope upset. Notice the minor perturbations in the error - the estimator rapidly converges back to an estimate with error on the order of 10^{-4}.

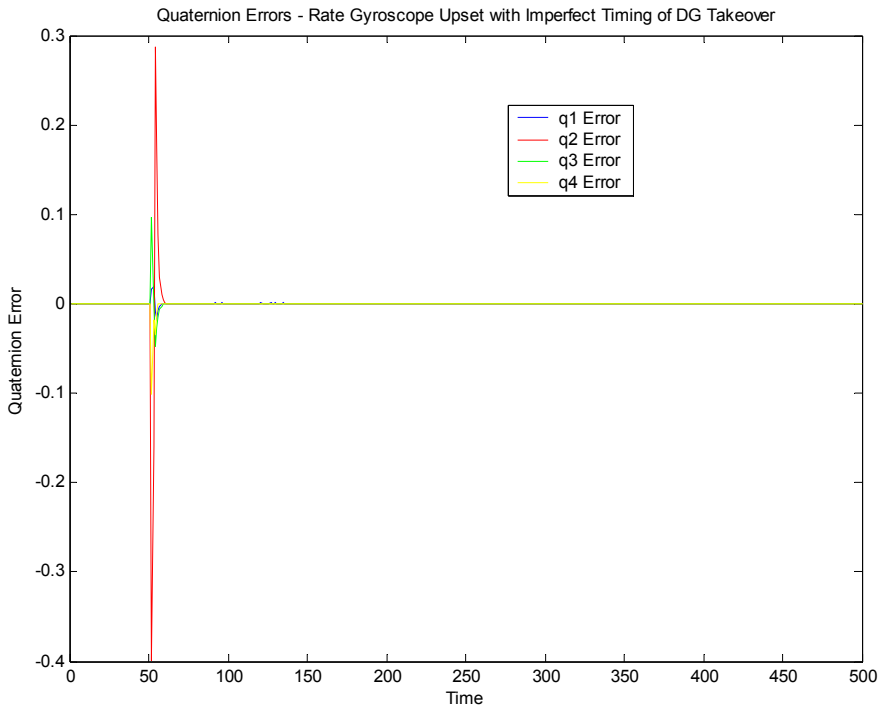

Figure 21. Quaternion Error with Dynamic Gyroscope Takeover Occurring Two Seconds after Rate Gyroscope Upset Commencement

By creating a switching algorithm with a high reliability, rate gyroscope upsets may be experienced by an attitude estimator using a Gibbs parameter based Kalman filter with little loss of estimator accuracy, as can be seen in the figures above.

THIS PAGE INTENTIONALLY LEFT BLANK

VI. CONCLUSIONS

The Gibbs parameter formulation of the Kalman filter provides an accurate estimate of spacecraft attitude. It is far more robust an estimator when confronted with either a star gap or rate gyroscope upset than the Euler angle estimator.

A. SUMMARY

A Kalman filter based upon the Gibbs parameterization of spacecraft attitude is developed and analyzed. A comparison between this formulation and a Kalman filter developed by Palermo is conducted under different operating scenarios. The dynamic gyroscope is shown to be a viable substitute for mechanical gyroscopes during periods of rate gyroscope upsets. The Gibbs parameter based Kalman filter used in conjunction with the dynamic gyroscope is shown to be an excellent method to mitigate the effects of rate gyroscope upsets and produces far superior results than the Euler angle formulation of the Kalman filter when faced with a rate gyroscope upset.

B. RECOMMENDATIONS

It is strongly recommended that future work be done on attitude estimation in two specific areas at a minimum: Kalman Filtering and Unscented Filtering.

1. Kalman Filtering

The Kalman filter developed in this work was limited to six states for purposes of the research. It is possible – and somewhat desirable in some cases – to have a much larger state vector estimating other factors impacting spacecraft attitude estimation such as scale factors of gyroscopes and star trackers, alignment errors in the sensor to body transformation matrices, misalignment of gyroscopes, and errors in the ECI to body coordinate transformations – among others. Grey, Kolve, Herman, and Westerlund have developed such a filter that is used in on-orbit calibrations [Gray]. The Aerospace Corporation has developed a similar filter. It is recommended that such filters and the modeling to support their implementation be developed and studied – implementing the Gibbs parameter formulation for attitude error estimation into these models.

2. Unscented Filtering

As mentioned in the description of the EKF, it is based upon a linearization of non-linear functions. This linearization is the fundamental flaw of the EKF. Julier et al

have developed an alternative to the EKF based on the premise that it should be easier to approximate a Gaussian distribution than to approximate an arbitrary non-linear function. Markley and Crassidis have adapted this filtering method to spacecraft attitude estimation and it is recommended that research into this method as an alternative to Kalman filtering be conducted [Crassidis].

LIST OF REFERENCES

1. Palermo, William J. *Angular Rate Estimation for Multi-Body Spacecraft Attitude Control*, Naval Postgraduate School Engineer's Thesis. June 2001.

2. Sidi, Marcel J., *Spacecraft Dynamics and Control: A Practical Engineering Approach*, Cambridge University Press, Melbourne, Australia, 1997.

3. Kolve, D. I., "Describing an Attitude", American Astronautical Society Paper, AAS 93-037, 6-10 February 1993.

4. Hewitson, S.A., Wang, J. Kearsley, A.H.W., *Performance Evaluation of Inertial Navigation Systems for Surveying*, 6th International Symposium on Satellite Navigation Technology Including Mobile Positioning & Location Services, Melbourne, Australia July 2003.

5. Wertz, J.R. and Larson, W. J.(editors). *Space Mission Analysis and Design, Third Edition*, Microcosm Press, El Segundo, CA. 1999.

6. Junkins, J. L., "Optical Navigation". Presentation at Naval Postgraduate School, November 2003.

7. Gray, C. W., Herman, L. K., Kolve, D. I., Westerlund, G. W., "On-Orbit Attitude Reference Alignment and Calibration", American Astronautical Society Paper, AAS 00-272, 20-21 March 2000.

8. Markley, F. Landis, "Attitude Error Representations for Kalman Filtering", *Journal of Guidance, Control, and Dynamics,* Vol. 26, No. 2, March-April 2003.

9. Crassidis, John L., Markley, F. Landis, "Unscented Filtering for Spacecraft Attitude Estimation", *Journal of Guidance, Control, and Dynamics*, Vol. 26, No. 4, July-... August 2003.

10. Wie, Bong, *Space Vehicle Dynamics and Control*, American Institute of Aeronautics and Astronautics, inc., Temple, AZ, 1998.

11. Hughes, Peter C. *Spacecraft Attitude Dynamics*. John Wiley and Sons, Incorporated, 1986.

THIS PAGE INTENTIONALLY LEFT BLANK

INITIAL DISTRIBUTION LIST

1. Defense Technical Information Center
   Ft. Belvoir, VA

2. Dudley Knox Library
   Naval Postgraduate School
   Monterey, CA

3. Department Chairman, Code AA
   Department of Aeronautics and Astronautics
   Naval Postgraduate School
   Monterey, CA

4. Professor Brij N. Agrawal, Code AA/Ag
   Department of Aeronautics and Astronautics
   Naval Postgraduate School
   Monterey, CA

5. Professor Roberto Cristi, Code EC/Cr
   Department of Electrical and Computer Engineering
   Naval Postgraduate School
   Monterey, CA

6. Professor Barry Leonard, Code AA/Ln
   Department of Aeronautics and Astronautics
   Naval Postgraduate School
   Monterey, CA

7. SRDC Research Library, Code AA
   Department of Aeronautics and Astronautics
   Naval Postgraduate School
   Monterey, CA